Autors response to referee 1

November 7, 2022

We thank reviewer 1 for his/her constructive comments on our technical note. We provide a detailed response in the text below, where the R1 comments are marked in blue, our response in black. Changes in the revised manuscript are in magenta for referee 1 and in blue for referee 2.

Comment: In their paper "Accelerated photosynthesis routine in LPJmL4" the authors show that using a different algorithm in a subroutine of the photosyntheis computation leads to model speed up and higher numerical accuracy of the DGVM LPJmL. I very much agree with the authors that DGVMs need improvements in their numerical methods to decrease their computing time. Therefore, I see the proposed methodology as an important step towards this goal.
Response: We are grateful that the reviewer supports our argument on improving numerical methods by which the computational time and numerical accuracy for key routines that form the core of Dynamic Global Vegetation Models are improved. Given the fact that first versions of DGVMs were published in the late 1990ies and early 2000s, it becomes necessary to revisit the methods of existing core routines from which many other modelled processes in the model depend.

Comment: However, I find that replacing the bisection method with the Newton method to find the root of a continuous function does not suffice for a technical paper. A short technical comment could be appropriate, but quite frankly I believe that this (nonetheless important) improvement of LPJmL should simply be mentioned in the release notes of a new release of LPJmL.
Response: We agree that the extend of the study shown here is comparably small in relation to other model development papers. However, we would like to stress that we use the implementation of the Newton method exemplarily to show and underline the necessity on how mathematical knowledge can be used to revisit and improve existing routines in models that are now continuously developed and applied in, e.g., climate change studies, for nearly two decades. Moreover, we think that these aspects do not receive enough attention in publications of larger model update papers, which serve different objectives.

Comment: I also find that important things are not sufficiently discussed, namely: 1. There are only two citations when mentioning that this representation of photosynthesis is used in the majority of DGVMs. There are also other representations of PS and more citations will underline the point that Farquhar-Collatz is really the most used one.
Response: We thank the reviewer for pointing out that the references are not complete. Reviewer 2 had made a similar remark. We therefore refer to our respective author response. (The additional text in the revised manuscript is in blue.)

2. It should at least be mentioned that the function f suffices all criteria for the Newton-method
Response: The Newton method requires that f is at least three times differentiable and the

first derivative of f at the iteration is not zero. We now explain this in the text (in magenta in the revised manuscript) and the sentence now reads:
The function f is defined for all $\lambda > 0$, as long as $(J_E(\lambda) + J_C(\lambda))^2 \geq 4\theta J_E(\lambda)J_C(\lambda)$. As a composition of at least three times differentiable functions it fulfills the differentiability condition of Newton's method.
The condition $f'(\lambda) \neq 0$ as well as the suitability of a staring value can not be generally ensured. In all our computations convergence was not a problem. To be on the safe side, one can implement a hybrid method that switches to bisection if convergence of the iterates does not occur.

3. Actually also a plot of f would be interesting to see, at least for one particular set of parameters, to let the reader get an impression of how this function looks like.

Response: We thank the reviewer for this helpful remark, as we agree that this additional plot helps to enhance the understanding of the function. We have identified the parameters that define the function f. Since some of these parameters vary with geographic location (average climate conditions) and season we have plotted them for a boreal, temperate and tropical site. All three sites are used as a standard in our model benchmarking. We have plotted f in a new Figure 1 and added the following text:
The parameters in the definition of f vary with the geographic location and season. A plot of f for parameters from different locations (boreal, temperate, and tropical) and at different times can be seen in Figure 1.

4. The Newton-method may fail when the starting value is chosen too far away from the root, it is not discussed whether this could become a problem.

Response: We discussed this comment in the text (see above): The condition $f'(\lambda) \neq 0$ as well as the suitability of a staring value can not be generally ensured. In all our computations convergence was not a problem. To be on the safe side, one can implement a hybrid method that switches to bisection if convergence of the iterates does no occur.

5. Some outputs had much higher changes when the new method was applied. There is no discussion why that could be.

Response: We have stressed that the changes appear larger but are of small dimension due to small absolute values. Since these occur in areas of low productivity for which reliable validation data are difficult to obtain, therefore hard to decide which version yields more reliable results. We also refer to our detailed response in our response to Reviewer 2, where we additionally tested the parameter sensitivity on annual GPP.

Comment: To conclude, I unfortunately cannot recommend this manuscript for publication as I evaluate its impact as too low for a paper in GMD.

Response: We hope that we have provided the required information and additional explanations that the revised manuscript would deserve publication as a technical note in GMD, also with the material added following review 2.

Autors response to referee 2

November 14, 2022

We thank reviewer 2 for his/her constructive comments on our technical note, especially for the detailed suggestions and suggested references which helped us to substantially improve our manuscript. We provide a detailed response in the text below, where the comments from Reviewer 2 are marked in blue, our responses in black. Changes in the revised manuscript are in magenta for referee 1 and in blue for referee 2.

This topic is generally appropriate for a report in Geoscientific Model Development, but as currently written the manuscript is likely to be relatively low impact. Primary concerns are: (1) the application of Newton's method to this problem while logical is not novel; (2) while it speeds the solution, the marginal improvement is modest (only on the order of 16%); (3) the focus on the acceleration of the photosynthesis scheme overlooks substantial underlying problems with calibration and evaluation of this scheme. To increase the impact of this manuscript, I would suggest: (a) including a concise review of the numeric methods used to implement the Farquhar-Collatz style photosynthesis schemes in land surface models; (b) better contextualizing the importance of computational efficiency relative to other priorities for the development of the photosynthesis scheme; (c) condensing the figures down to one or two key visuals, summarizing the magnitude of the impact of Newton's method.

(a) re concise review. We thank the reviewer for this thoughtful suggestion. It allows us to reflect recent scientific discussions around the Farquhar-Collatz photosynthesis scheme in our manuscript. Please see our response to the specific point related to this general issue further below, where we describe the inserted literature review.

(b) re importance of computational efficiency vs. improvements of parameter: we thank the reviewer for this important suggestion. We have now tested the most sensitive parameters in the photosynthesis routine thanks to the work published in [Walker et al. 2020] and describe the outcome in comparison to the effect of improving computation efficiency in the manuscript. See our detailed reply further below.

(c) re condensing figures: We understand that the figures which form part of our standard benchmarking protocol of the LPJmL model to measure model improvements and consistency was misleading. We wanted to show that the model is still robust, although it did not improve the simulation of general model variables such as carbon storage and fluxes. See also our response below regarding detailed evaluation of the photosynthesis scheme and parameter sensitivity.

Line 30, The current text should be updated to accurately describe the pathway that the Farquhar-style model took into large-scale applications. The Farquhar et al. (1980) photosynthesis model was originally coupled to a stomatal model by Collatz et al. (1991; 1992). The coupled photosynthesis-conductance scheme was then integrated into the Simple Biosphere

Model developed by Sellers et al. (1992; 1996a, b, c, d). These initial applications were then built on by [Haxeltine and Prentice(1996a), Haxeltine and Prentice(1996b)].
We thank the reviewer for this suggestion to go back in time and explain the originals of this scheme. It certainly helps to trace the genesis of the modelling approach. In fact as [Pitman 2003] described it with the inclusion of the coupled photosynthesis-transpiration scheme the 3rd generation of Land Surface Models was formed. On top of that a second line of development which is briefly mentioned in [Pitman 2003], but not sufficiently explained therein, is the group of Dynamic Global Vegetation Models (DGVMs). Some DGVMs were developed to be coupled to LSMs and embedded in AOGCMs or Earth System Models, others by design to be stand-alone models to project climate impacts on the land biosphere, namely vegetation dynamics interacting with carbon, water and energy fluxes [Prentice et al.(2007)]. Many DGVMs also use the Farquhar-Collatz photosynthesis scheme which was developed further in Haxeltine and Prentice [Haxeltine and Prentice(1996a)] and then implemented in the BIOME-3 model [Haxeltine and Prentice(1996b)]. Since then more DGVMs have build up their photosynthesis schemes on those early publications so that today's DGVMs use this scheme to a large extent. Because a similar comment on providing a complete overview on the DGVMs using the Farquhar-Collatz photosynthesis scheme was made by Reviewer 1, we now added this overview in the newly added 2 paragraphs which review the respective literature on both lines of model development from line 33:
"The Farquhar-Collatz approach was implemented in the land surface of the SiB2 model by [Sellers et al.(1992), Sellers et al.(1996a)] where it replaced their empirical photosynthesis model. The photosynthesis model in SiB2 [Sellers et al.(1996b)] covers the co-limitation by Rubisco enzyme activity, light availability and export limitation of carbon compounds. Furthermore, it covers the gradient between inner-stomatal CO_2 concentration to the CO_2 concentration around the leaf surface in the computation of stomatal conductance. By implementing the semi-mechanistic photosynthesis model and coupling it to transpiration via stomatal conductance, the LSM could then not only investigate biophysical effects of climate change but also biogeochemical effects of rising atmospheric CO_2 in the Earth System [Pitman 2003]. The SiB2 model [Sellers et al.(1992), Sellers et al.(1996a)], the NCAR CCM2 model [Bonan et al. 1995], and the MOSES land surface model of the UK Met office [Cox et al. 1998] were among the first to implement this photosynthesis scheme and evaluated it against field campaigns. Today, the Farquhar-Collatz photosynthesis model is used in a number of Land surface models of the CMIP-5 Earth System Models, such as the Community Atmosphere Biosphere Land Exchange (CABLE) LSM of the Australian Community Climate Earth system Simulator (ACCESS, see [de Kauwe et al. 2015], and ref. therein) as well as the ORCHIDEE DGVM [Krinner et al.(2005)] of the IPSL-CM5 Earth System Model [Dufresne et al. 2013]. Different models of stomatal conductance were evaluated for the JSBACH LSM [Reick et al. 2013] of the Max Planck Institute Earth System Model (MPI-ESM) to account for hydraulic properties and drought response [Knauer et al. 2015]. The Community Land Model CLM4.5 [Oleson et al. 2013] of the NCAR ESM use the Ball-Berry model of stomatal conductance and extended it to account for leaf temperature acclimation and leaf water potential [Bonan et al. 2014]; a similar approach was implemented in the JULES-vn5.6 land surface model [Oliver et al. 2022] of the UK Hadley Centre ESM [Sellar et al. 2019].
While Land surface models detail vertical water, energy and carbon profiles within the canopy, which extrapolates the photosynthetic capacity calculated at the leaf level to canopy photosynthesis [Sellers et al.(1996b)], stand-alone DGVMs often use a big-leaf approach and compute daytime photosynthesis for canopy conductance which goes back to the BIOME-3 model [Haxeltine and Prentice(1996b)] which opened up the second line of vegetation models by embedding the Farquhar-Collatz photosynthesis model in a modelling framework of plant physiology and vegetation dynamics in DGVMs [Prentice et al.(2007)]. The [Haxeltine and Prentice(1996b)] implementation is used in the LPJ model family originating from [Sitch et al. (2003)] and the LPJ-GUESS model [Smith et al. 2001, Smith et al. 2014], as well as the current LPJmLv4 model [Schaphoff et al.(2018a), Schaphoff et al.(2018b)]. Today, 14 DGVMs (stand-alone and coupled to land-surface models) contribute to the TRENDY intercomparison project

(https://blogs.exeter.ac.uk/trendy/) that informs the global carbon project on the state of the land carbon sink [Sitch et al. 2015]."

Lines 37-38, I recognize that some of this will be presented later, but it would help to set up the manuscript to summarize the runtime analysis here and state what fraction of the total time was originally required by the photosynthesis routine.
We compiled LPJmL using the -pg option to allow profiling. We executed the model for one grid cell to obtain the profile output from which the table on runtimes was produced using the gprof utility. The table contains the number of self calls and cumulative seconds as well as percentages of the runtime each routine required. It turned out that the photosynthesis routine using the bisection method required 38 per cent of the total computation time. The updated sentence now reads: "We quantified the runtime required by each submodule (or routine) of the LPJmL DGVM using the profiling option of the compilation command and the linux gprof utility. We found that the repeated execution of the photosynthesis routine demands a big fraction, i.e. 38%, of the computational time. All other routines require less than 11%."

Lines 42-45, Suggest to review and summarize here the literature on the numeric methods that have been used to implement the Farquhar-Collatz style photosynthesis schemes within land surface models. Newton's method has been implemented in many different modeling frameworks to solve the coupled photosynthesis-conductance-energy balance schemes, but I am not aware of a review that provides a concise overview of these applications.
We thank the reviewer for suggesting to provide such an overview in land surface schemes. We would have assumed that the exact numerical methods used would be documented in the peer-reviewed literature to provide a concise overview on the use of Newton's method in different modelling frameworks to solve coupled balance schemes. We were surprised to find very few additional references in the published literature. We searched the peer-reviewed data base Web of Science and also Google Scholar (using the keyword combination Farquhar AND photosynthesis AND Newton) and it seems these methods were rarely documented in the peer-reviewed literature. When working on the implementation of the Newton scheme for the photosynthesis, we found the hint in [Collatz et al. 1991], p.119, that the Newton method was used, but no documentation on the mathematical implementation, its computational cost or respective model code was provided. The same holds for [Pearcy et al. 1997] who looked at light regulation of two species at the leaf level. We found a description of photosynthesis model for rose leaf [Soo-Hyung and Lieth 2003], where the authors stated the use of the Newton-Raphson method to compute λ, but again no formulas or code were provided. In [Dubois et al. 2007] the statistical estimation of the parameters of the Farquhar-Collatz model is optimized by simultaneous estimation of multiple segments. For the required nonlinear regressions iterative methods like Gauss-Newton, steepest descent, or Levenberg-Marquardt algorithm are proposed. Again, there is no documentation. From the code in the supplements one can derive that Levenberg-Marquardt method was used. [Bonan et al. 2014] mentions numerical solution methods in their approach to include leaf water potentials, but again no details on this particular aspect are provided. This supports our view that the documentation and implementation of such a methods should be provided at least once.
We now refer to those references in the text: "Only a few, detailed specialized studies mention the use of Newton's or similar methods to solve coupled balance schemes, [Collatz et al. 1991, Pearcy et al. 1997, Soo-Hyung and Lieth 2003, Dubois et al. 2007], or extensions of the photosynthesis-transpiration scheme along the leaf-plant-soil continuum in DGVMs [Bonan et al. 2014] are mentioned, but none provide a documentation on the computational efficiency, or how the numerical method was implemented in the model and/or a code."

Lines 99-129, Section is difficult to follow without having the mathematical symbols defined at first use and the flow of the equations explained in narrative form. To improve readability, suggest defining each mathematical symbol in text at first use and also explaining what each

equation represents in physical terms rather than just presenting the mathematical derivation.
We followed the suggestions of the referee and defined each symbol in the text (We still kept the table of symbols in the appendix). Each term of the defined function f is now physically explained and some additional remarks were added that should make it easier to follow the computation of the derivative of f.

Lines 174-184, The argument developed here is a bit confusing. The lack of an impact of Newton's method on modeled pools and fluxes does not imply anything about the accuracy of the pool/flux calculations. The "accuracy of the photosynthesis scheme" must be defined relative to skill at explaining observations. Recent work by Walker et al. has highlighted the challenges in rigorously confronting the Farquhar-Collatz style schemes with observations due to the empirical coefficients that have been used as tuning knobs. One path forward is updating the current Farquhar-Collatz approach with the Johnson and Berry (2021) scheme which eliminates empirical coefficients, reduces the total number of free variables, and permits calculation of both gas-exchange and chlorophyll fluorescence.
Thanks for this valuable comment which helps to improve our manuscript substantially. Although it is possible to replace the Farquhar-Collatz scheme by the Johnson and Berry scheme [Johnson and Berry 2021], after intensive discussion we came to the conclusion that such an implementation into the LPJmL photosynthesis scheme is currently out of scope for this study. We now mention this step as a possible future development in our discussion section, were we state: "Future work on the photosynthesis approach could focus on the new Johnson and Berry scheme [Johnson and Berry 2021] with the advantage of calculating gas-exchange and relying less on empirical coefficients".

Instead, we have intensively studied the [Walker et al. 2020] paper and following their findings we have tested the influence of the following parameters wrt their sensitivity on GPP: $\theta, \alpha_{C3}, b_{C3}, k_{c25}, K_{o25}$ on changes to GPP. Although [Walker et al. 2020] have identified V_{cmax} to be also a sensitive parameter in the photosynthesis scheme ([Walker et al. 2020], see Table 2 therein for V_{cmax} parameter range), the way the Farquhar-Collatz approach is implemented in LPJmL does not allow to specify V_{cmax} as a parameter. The LPJmL model computes V_m as follows [Schaphoff et al.(2018a)], eq. (35):

$$V_m = \frac{1}{b_{C3}} \cdot \frac{c_1}{c_2} \cdot ((2\theta - 1) * s - (2\theta * s - c_2) * \sigma) \cdot APAR.$$

Therefore, the sensitivity of V_{cmax} results from varying b_{C3} indirectly since the reciprocal of b_{C3} is used to calculate V_{cmax} in a linear equation. Varying b_{C3} is therefore the adequate sensitivity test which relates to V_{cmax}. We have now inserted the following text in the manuscript:
"In addition to improving the computational efficiency and numerical precision, parameter uncertainties have been tested by [Walker et al. 2020], who tested the sensitivity of $\theta, \alpha_{C3}, b_{C3}, k_{c25}, K_{o25}$ on their impacts on global GPP. The LPJmL model computes V_m as follows [Schaphoff et al.(2018a)], eq. (35):

$$V_m = \frac{1}{b_{C3}} \cdot \frac{c_1}{c_2} \cdot ((2\theta - 1) * s - (2\theta * s - c_2) * \sigma) \cdot APAR.$$

Therefore, the sensitivity of V_{cmax} results from varying b_{C3} indirectly since the reciprocal of b_{C3} is used to calculate V_{cmax} in a linear equation. Varying b_{C3} is therefore the adequate sensitivity test which relates to V_{cmax}. We varied each parameter by 10% independently and find that θ ($\alpha_{C3}, b_{C3}, k_{c25}, K_{o25}$) increases global annual GPP (AGPP, hereafter) by 1.67% (+6.69%, -1.67%, -0.35%, +0.14%). Table 1 shows the difference of the two most important parameter on global AGPP.

parameter	Δ GPP relativ in %	Δ GPP absolut (GtC/yr)
θ	1.67	2.384
α_{C3}	6.68	9.542
b_{C3}	-0.56	-0.798
k_{c25}	-0.35	-0.506
K_{o25}	0.14	0.199

Table 1: Change in the AGPP after varying parameters by 10%.

Geographically, increasing θ yields higher AGPP mainly in the tropics and temperate forest regions, where AGPP increases up to 100 gC/m^2. However, AGPP increases between 200 and 500 gC/m^2 when changing α_{C3}, see Fig.1. It turns out that AGPP is increased in all regions, where LPJmL simulates woody PFTs. Also here, largest effects are seen in (sub-)tropical and temperate regions which span larger areas than the areas with increased AGPP as a result of varying θ."

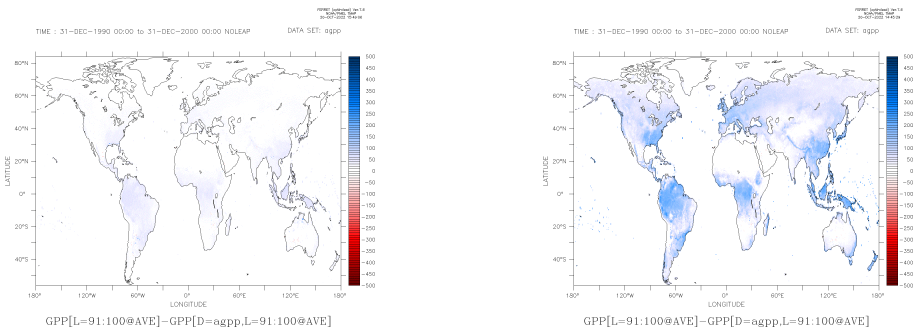

Figure R 1: Parameter sensitivity on Annual Gross Primary Productivity (AGPP) shown as the difference between the new parameter and the reference simulation. Both simulations have the Newton approach implemented. Increasing θ by 10 % increased AGPP mainly in forested regions (left panel). Increasing α_{C3} by 10 % has a much larger effect on AGPP, especially in the tropics (right panel).

We have now inserted the additional sensitivity test as a new paragraph, and include figure R 1 as the new Figure 4.

Figures D1-D12, The current figures simply summarize differences in model output across a variety of metrics; they add relatively little to the impact of the paper and it would be useful to distill them down to a smaller number of key visuals.

We understand that by showing the robustness of model simulations which are built on our benchmarking model evaluation system, we do not sufficiently display the main differences of the Newton approach and the parameter sensitivity. With the benchmarking we compare new model developments to a reference, i.e. master version. Because LPJmL has grown into a complex multi-sectorial model, we thought it to be important to show that the model is robust. We understand that this is not informative to the wider readership and show now only the figures related to GPP/NPP, vegetation carbon (i.e. biomass) and transpiration (because of the link via stomatal conductance) in terms of difference maps and only for NPP and transpiration as the global time series. This way, we have cut the number of figures by half.

References

[Farquhar et al. 1980] Farquhar, G. D., von Caemmerer, S., and Berry, J. A. (1980). A biochemical model of photosynthetic CO2 assimilation in leaves of C3 species. Planta, 149(1), 78–90. https://doi.org/10.1007/BF003 86231

[Walker et al. 2020] Walker, AP, Johnson, AL, Rogers, A, Anderson, J, Bridges, R.A., Fisher, R.A., Lu, D., Ricciuto, D.M., Serbin, S.P., Ye, M. Multi-hypothesis comparison of Farquhar and Collatz photosynthesis models reveals the unexpected influence of empirical assumptions at leaf and global scales. Glob Change Biol. 2021; 27: 804– 822. https://doi.org/10.1111/gcb.15366

[Collatz et al. 1991] Collatz, G.J., Ball, J.T., Grivet, C. and Berry, J.A.: Physiological and environmental regulation of stomatal conductance, photosynthesis and transpiration: a model that includes a laminar boundary layer. Agric. For. Meteorol,, 54: 107-136, https://doi.org/10.1016/0168-1923(91)90002-8, 1991.

[Collatz et al. 1992] Collatz GJ , Ribas-Carbo M Berry JA (1992) Coupled Photosynthesis-Stomatal Conductance Model for Leaves of C4 Plants. Functional Plant Biology 19, 519-538. https://doi.org/10.1071/PP9920519

[Pitman 2003] Pitman, A.J. (2003), The evolution of, and revolution in, land surface schemes designed for climate models. Int. J. Climatol., 23: 479-510. https://doi.org/10.1002/joc.893

[Prentice et al.(2007)] Prentice, I. C., Bondeau, A., Cramer, W., Harrison, S. P., Hickler, T., Lucht, W., Sitch, S., Smith, B., and Sykes, M. T.: Dynamic global vegetation modelling: quantifying terrestrial ecosystem responses to large-scale environmental change. In: Canadell, J.G., Pataki, D. E., and Pitelka L. F. (Eds.),Terrestrial Ecosystems in a Changing World, Springer, Springer Nature, https://doi.org/10.1007/978-3-540-32730-1, 2007.

[Haxeltine and Prentice(1996a)] Haxeltine, A., and Prentice, I. C.: BIOME3: An equilibrium terrestrial biosphere model based on ecophysiological constraints, resource availability, and competition among plant functional types, Global Biogeochemical Cycles, 10, 693-709, https://doi.org/10.1029/96GB023441996.

[Haxeltine and Prentice(1996b)] Haxeltine, A., and Prentice, I. C.: A general model for the light-use efficiency of primary production, Functional Ecology, 10, 551-561, https://doi.org/10.2307/2390165, 1996.

[Sellers et al.(1992)] Sellers, P.J., Berry, J.A., Collatz, G.J., Field, C.B. and Hall, F.G., 1992. Canopy reflectance, photosynthesis, and transpiration. III. A reanalysis using improved leaf models and a new canopy integration scheme. Remote sensing of environment, 42(3), pp.187-216.

[Sellers et al.(1996a)] Sellers, P.J., Randall, D.A., Collatz, G.J., Berry, J.A., Field, C.B., Dazlich, D.A., Zhang, C., Collelo, G.D. and Bounoua, L., 1996. A revised land surface parameterization (SiB2) for atmospheric GCMs. Part I: Model formulation. Journal of climate, 9(4), pp.676-705.

[Sellers et al.(1996b)] Sellers, P.J., Tucker, C.J., Collatz, G.J., Los, S.O., Justice, C.O., Dazlich, D.A. and Randall, D.A., 1996. A revised land surface parameterization (SiB2) for atmospheric GCMs. Part II: The generation of global fields of terrestrial biophysical parameters from satellite data. Journal of climate, 9(4), pp.706-737.

[Bonan et al. 1995] Bonan GB. 1995. Land–atmosphere CO2 exchange simulated by a land surface process model coupled to an atmospheric general circulation model. Journal of Geophysical Research 100: 2817–2831.

[Cox et al. 1998] Cox PM, Huntingford C, Harding RJ. 1998. A canopy conductance and photosynthesis model for use in a GCM land surface scheme. Journal of Hydrology 212–213: 79–94.

[de Kauwe et al. 2015] De Kauwe, M. G., Kala, J., Lin, Y.-S., Pitman, A. J., Medlyn, B. E., Duursma, R. A., Abramowitz, G., Wang, Y.-P., and Miralles, D. G.: A test of an optimal stomatal conductance scheme within the CABLE land surface model, Geosci. Model Dev., 8, 431–452, https://doi.org/10.5194/gmd-8-431-2015, 2015

[Krinner et al.(2005)] Krinner, G., Viovy, N., Noblet-Ducoudré, N. d., Ogée, J., Polcher, J., Friedlingstein, P., Ciais, P., Sitch, S., and Prentice, I. C.: A dynamic global vegetation model for studies of the coupled atmosphere-biosphere system, Global Biogeochemical Cycles, 19, https://doi.org/10.1029/2003GB002199, 2005.

[Dufresne et al. 2013] Dufresne, JL., Foujols, MA., Denvil, S. et al. Climate change projections using the IPSL-CM5 Earth System Model: from CMIP3 to CMIP5. Clim Dyn 40, 2123–2165 (2013). https://doi.org/10.1007/s00382-012-1636-1

[Reick et al. 2013] Reick, C., T. Raddatz, V. Brovkin, and V. Gayler (2013), Representation of natural and anthropogenic land cover change in MPI-ESM, J. Adv. Model. Earth Syst., 5, 459–482, doi:10.1002/jame.20022.

[Knauer et al. 2015] Knauer, J., Werner, C., and Zaehle, S. (2015), Evaluating stomatal models and their atmospheric drought response in a land surface scheme: A multibiome analysis, J. Geophys. Res. Biogeosci., 120, 1894– 1911, doi:10.1002/2015JG003114.

[Oleson et al. 2013] Oleson, K. W., Lawrence, D. M., Bonan, G. B., Drewniak, B., Huang, M., Koven, C. D., Levis, S., Li, F., Riley, W. J., Subin, Z. M., Swenson, S. C., Thornton, P. E., Bozbiyik, A., Fisher, R., Heald, C. L., Kluzek, E., Lamarque, J.-F., Lawrence, P. J., Leung, L. R., Lipscomb, W., Muszala, S., Ricciuto, D. M., Sacks, W., Sun, Y., Tang, J., and Yang, Z.-L.: Technical description of version 4.5 of the Community Land Model (CLM), NCAR Tech. Note NCAR/TN-503+STR, National Center for Atmospheric Research, Boulder, Colorado, 420 pp., 2013.

[Bonan et al. 2014] Bonan, G. B., Williams, M., Fisher, R. A., and Oleson, K. W.: Modeling stomatal conductance in the earth system: linking leaf water-use efficiency and water transport along the soil–plant–atmosphere continuum, Geosci. Model Dev., 7, 2193–2222, https://doi.org/10.5194/gmd-7-2193-2014, 2014

[Oliver et al. 2022] Oliver, R. J., Mercado, L. M., Clark, D. B., Huntingford, C., Taylor, C. M., Vidale, P. L., McGuire, P. C., Todt, M., Folwell, S., Shamsudheen Semeena, V., and Medlyn, B. E.: Improved representation of plant physiology in the JULES-vn5.6 land surface model: photosynthesis, stomatal conductance and thermal acclimation, Geosci. Model Dev., 15, 5567–5592, https://doi.org/10.5194/gmd-15-5567-2022, 2022

[Sellar et al. 2019] Sellar, A. A., Jones, C. G., Mulcahy, J. P., Tang, Y., Yool, A., Wiltshire, A., O'Connor, F. M., Stringer, M., Hill, R., Palmieri, J., Woodward, S., de Mora, L., Kuhlbrodt, T., Rumbold, S. T., Kelley, D. I., Ellis, R., Johnson, C. E., Walton, J., Abraham, N. L., Andrews, M. B., Andrews, T., Archibald, A. T., Berthou, S., Burke, E., Blockley, E., Carslaw, K., Dalvi, M., Edwards, J., Folberth, G. A., Gedney, N., Griffiths, P. T., Harper, A. B., Hendry, M. A., Hewitt, A. J., Johnson, B., Jones, A., Jones, C. D., Keeble, J., Liddicoat, S., Morgenstern, O., Parker, R. J., Predoi, V., Robertson, E., Siahaan, A., Smith, R. S., Swaminathan, R., Woodhouse, M. T., Zeng, G., and Zerroukat, M.: UKESM1: Description and Evaluation of the U.K. Earth System Model, J. Adv. Model. Earth Sy., 11, 4513–4558, https://doi.org/10.1029/2019MS001739, 2019.

[Prentice et al.(2007)] Prentice, I. C., Bondeau, A., Cramer, W., Harrison, S. P., Hickler, T., Lucht, W., Sitch, S., Smith, B., and Sykes, M. T.: Dynamic global vegetation modelling:

quantifying terrestrial ecosystem responses to large-scale environmental change. In: Canadell, J.G., Pataki, D. E., and Pitelka L. F. (Eds.),Terrestrial Ecosystems in a Changing World, Springer, Springer Nature, https://doi.org/10.1007/978-3-540-32730-1, 2007.

[Sitch et al. (2003)] Sitch, S., Smith, B., Prentice, I. C., Arneth, A., Bondeau, A., Cramer, W., Kaplan, J. O., Levis, S., Lucht, W., Sykes, M. T., Thonicke, K., and Venevsky, S.: Evaluation of ecosystem dynamics, plant geography and terrestrial carbon cycling in the LPJ dynamic global vegetation model, Global Change Biology, 9, 161-185, 10.1046/j.1365-2486.2003.00569.x, 2003.

[Smith et al. 2001] Smith, B., Prentice, I.C., and Sykes, M.T. 2001. Representation of vegetation dynamics in modelling of terrestrial ecosystems: comparing two contrasting approaches within European climate space. Global Ecology and Biogeography 10: 621-637.

[Smith et al. 2014] Smith, B., Wårlind, D., Arneth, A., Hickler, T., Leadley, P., Siltberg, J., and Zaehle, S.: Implications of incorporating N cycling and N limitations on primary production in an individual-based dynamic vegetation model, Biogeosciences, 11, 2027–2054, https://doi.org/10.5194/bg-11-2027-2014, 2014

[Schaphoff et al.(2018a)] Schaphoff, S., von Bloh, W., Rammig, A., Thonicke, K., Biemans, H., Forkel, M., Gerten, D., Heinke, J., Jägermeyr, J., Knauer, J., Langerwisch, F., Lucht, W., Müller, C., Rolinski, S., and Waha, K.: LPJmL4 - a dynamic global vegetation model with managed land, Part 1: Model description, Geoscientific Model Development, 11, 1343-1375, https://doi.org/10.5194/gmd-11-1377-2018, 2018.

[Schaphoff et al.(2018b)] Schaphoff, S., Forkel, M., Müller, C., Knauer, J., von Bloh, W., Gerten, D., Jägermeyr, J., Lucht, W., Rammig, A., Thonicke, K., and Waha, K.: LPJmL4 - A dynamic global vegetation model with managed land, Part 2: Model evaluation, Geoscientific Model Development, 11, 1377-1403, https://doi.org/10.5194/gmd-11-1377-2018, 2018.

[Sitch et al. 2015] Sitch, S., Friedlingstein, P., Gruber, N., Jones, S. D., Murray-Tortarolo, G., Ahlström, A., Doney, S. C., Graven, H., Heinze, C., Huntingford, C., Levis, S., Levy, P. E., Lomas, M., Poulter, B., Viovy, N., Zaehle, S., Zeng, N., Arneth, A., Bonan, G., Bopp, L., Canadell, J. G., Chevallier, F., Ciais, P., Ellis, R., Gloor, M., Peylin, P., Piao, S. L., Le Quéré, C., Smith, B., Zhu, Z., and Myneni, R.: Recent trends and drivers of regional sources and sinks of carbon dioxide, Biogeosciences, 12, 653–679, https://doi.org/10.5194/bg-12-653-2015, 2015

[Pearcy et al. 1997] Pearcy, R.W., Gross, L.J. and HE, D., An improved dynamic model of photosynthesis for estimation of carbon gain in sunfleck light regimes. Plant, Cell and Environment, 20: 411-424. https://doi.org/10.1046/j.1365-3040.1997.d01-88.x, 1997.

[Soo-Hyung and Lieth 2003] Soo-Hyung Kim, Lieth, J.H., A Coupled Model of Photosynthesis, Stomatal Conductance and Transpiration for a Rose Leaf (Rosa hybrida L.), Annals of Botany, Volume 91(7): 771–781, https://doi.org/10.1093/aob/mcg080, 2003

[Dubois et al. 2007] Dubois, J.-J.B., Fiscus, E.L., Booker, F.L., Flowers, M.D. and Reid, C.D., Optimizing the statistical estimation of the parameters of the Farquhar–von Caemmerer–Berry model of photosynthesis. New Phytologist, 176: 402-414. https://doi.org/10.1111/j.1469-8137.2007.02182.x, 2007

[Johnson and Berry 2021] Johnson, J.E. and Berry, J.A.: The role of cytochrome b6f in the control of steady- state photosynthesis: a conceptual and quantitative model. Photosynthesis Research, 148(3), pp.101-136, 2021

Accelerated photosynthesis routine in LPJmL4

Jenny Niebsch[1], Werner von Bloh[2], Kirsten Thonicke[2], and Ronny Ramlau[1]

[1]RICAM, Altenbergerstr. 69, 4040 Linz, Austria

[2]Potsdam Institute for Climate Impact Research (PIK), Member of the Leibniz Association, 14412 Potsdam, Germany

Correspondence: Jenny Niebsch (jenny.niebsch@oeaw.ac.at)

Abstract. The increasing impacts of climate change require strategies for climate adaptation. Dynamic Global Vegetation Models (DGVMs) are one type of multi-sectorial impact models with which the effects of multiple interacting processes in the terrestrial biosphere under climate change can be studied. The complexity of DGVMs is increasing as more and more processes, especially for plant physiology, are implemented. Therefore, there is a growing demand for increasing the computational performance of the underlying algorithms as well as ensuring their numerical accuracy. One way to approach this issue is to analyse the routines which have the potential for improved computational efficiency and/or increased accuracy when applying sophisticated mathematical methods.

In this paper, the Farquhar-Collatz photosynthesis model under water stress as implemented in the Lund-Potsdam-Jena managed Land DGVM (4.0.002) was examined. We additionally tested the uncertainty of most important parameter on photosynthesis as an additional approach to improve model quality. We found that the numerical solution of a nonlinear equation, so far solved with the Bisection method, could be significantly improved by using Newton's method instead. The latter requires the computation of the derivative of the underlying function which is presented. Model simulations show a significant lower number of iterations to solve the equation numerically and an overall run time reduction of the model of about 16 $\%$ depending on the chosen accuracy. Increasing the parameters θ and α_{C3} by 10 $\%$, respectively, while keeping all other parameter at their original value, increased global GPP by 2.384 GtC/yr and 9.542 GtC/yr, respectively. The Farquhar-Collatz photosynthesis model forms the core component in many DGVMs and land-surface models. An update in the numerical solution of the nonlinear equation in connection with adjusting globally important parameter to best known values, can therefore be applied to similar photosynthesis models. Furthermore, this exercise can serve as an example for improving computationally costly routines while improving their mathematical accuracy.

1 Introduction

Climate change is increasingly affecting the world we live in and that in turn affects nature's contribution to our livelihoods, (Pörtner et al., 2022). Estimating the extent and impacts of climate change has become more and more urgent over the last couple of decades. Earth System models as well as impact models are used to develop strategies for climate adaptation and mitigation to achieve the Paris climate accord, (Masson-Delmotte et al., 2021), (Pörtner et al., 2022). Climate change affects vegetation dynamics, biodiversity, water and biogeochemical cycles which could reduce the biosphere's capacity to absorb carbon from the atmosphere in the future. Dynamic Global Vegetation Models (DGVMs) are applied to study the net effects of

multiple interacting processes that affect carbon sequestration (photosynthesis) and storage (in biomass and soil), see (Prentice et al., 2007). It shows the demand for reliable and consistent model projections which require continuous work on reducing model uncertainty. While increasing complexity of the models by including more and more processes in DGVMs has been matched by increasing high-performance computing capabilities over the past decades, little has been invested in identifying and optimizing computationally intensive routines in the model (Reichstein et al., 2019). These routines often have a long model history as they frequently belong to the core routines stemming from the very first model version. This includes, e.g., the physiological modelling core of simulating photosynthesis in connection with atmospheric water demand or plant-water stress. The photosynthesis model is based on the Farquhar approach implemented in first global biome models by Haxeltine and Prentice (1996a) from which DGVMs evolved later on, (Prentice et al., 2007). Today, this type of photosynthesis module forms the core of the majority of DGVMs, see e.g., (Smith et al., 2001, 2014; Krinner et al., 2005).

The Farquhar-Collatz approach was implemented in the land surface of the SiB2 model by Sellers et al. (1992, 1996a) where it replaced their empirical photosynthesis model. The photosynthesis model in SiB2 (Sellers et al., 1996b) covers the co-limitation by Rubisco enzyme activity, light availability and export limitation of carbon compounds. Furthermore, it covers the gradient between inner-stomatal CO_2 concentration to the CO_2 concentration around the leaf surface in the computation of stomatal conductance. By implementing the semi-mechanistic photosynthesis model and coupling it to transpiration via stomatal conductance, the LSM could then not only investigate biophysical effects of climate change but also biogeochemical effects of rising atmospheric CO_2 in the Earth System (Pitman, 2003). The SiB2 model (Sellers et al., 1992, 1996a), the NCAR CCM2 model (Bonan et al. , 1995), and the MOSES land surface model of the UK Met office (Cox et al., 1998) were among the first to implement this photosynthesis scheme and evaluated it against field campaigns. At present, the Farquhar-Collatz photosynthesis model is used in a number of Land surface models of the CMIP-5 Earth System Models, such as the Community Atmosphere Biosphere Land Exchange (CABLE) LSM of the Australian Community Climate Earth system Simulator (ACCESS, see (de Kauwe et al., 2015), and ref. therein) as well as the ORCHIDEE DGVM (Krinner et al., 2005) of the IPSL-CM5 Earth System Model (Dufresne et al., 2013). Different models of stomatal conductance were evaluated for the JSBACH LSM (Reick et al., 2013) of the Max Planck Institute Earth System Model (MPI-ESM) to account for hydraulic properties and drought response (Knauer et al., 2015). The Community Land Model CLM4.5 (Oleson et al., 2013) of the NCAR ESM use the Ball-Berry model of stomatal conductance and extended it to account for leaf temperature acclimation and leaf water potential (Bonan et al. , 2014); a similar approach was implemented in the JULES-vn5.6 land surface model (Oliver et al., 2022) of the UK Hadley Centre ESM (Sellar et al., 2019).

While Land surface models detail vertical water, energy and carbon profiles within the canopy, which extrapolates the photosynthetic capacity calculated at the leaf level to canopy photosynthesis (Sellers et al., 1996b), stand-alone DGVMs often use a big-leaf approach and compute daytime photosynthesis for canopy conductance which goes back to the BIOME-3 model (Haxeltine and Prentice, 1996b) which opened up the second line of vegetation models by embedding the Farquhar-Collatz photosynthesis model in a modelling framework of plant physiology and vegetation dynamics in DGVMs (Prentice et al., 2007). The Haxeltine and Prentice (1996b) implementation is used in the LPJ model family originating from Sitch et al. (2003) and the LPJ-GUESS model (Smith et al., 2001, 2014), as well as the current LPJmLv4 model (Schaphoff et al., 2018a, b).

Today, 14 DGVMs (stand-alone and coupled to land-surface models) contribute to the TRENDY intercomparison project (https://blogs.exeter.ac.uk/trendy/) that informs the global carbon project on the state of the land carbon sink (Sitch et al., 2015).

In order to apply the model to the global land surface it is not anymore sufficient to use faster or larger computing infrastructure or try to parallelise the code as in von Bloh et al. (2010). It rather requires the evaluation of the underlying algorithm structure of the code, and in particular the used numerical methods. Replacing 'old' numerical algorithms by modern methods will result in a significantly better run-time performance while simultaneously maintaining or even increasing the accuracy of the method. We quantified the runtime required by each submodule (or routine) of the LPJmL DGVM using the profiling option of the compilation command and the linux gprof utility. We found that the repeated execution of the photosynthesis routine demands a big fraction, i.e. 38%, of the computational time. All other routines require less than 11%.

To illustrate our approach, our goal was to improve the computational efficiency of DGVMs by accelerating the photosynthesis module under water stress conditions using the Lund-Potsdam-Jena DGVM, (Schaphoff et al., 2018a, b), as an example. A key ingredient in the modelling of photosynthesis is the determination of the ratio λ between intracellular and ambient CO_2 concentration. Mathematically, λ is computed as a zero of a nonlinear equation $f(\lambda) = 0$, which has been so far solved by a simple bisection algorithm. We expected to improve the computational efficiency by applying one of the more sophisticated solution methods, namely Regula falsi, secant and Newton's method. In this technical paper, we describe testing all three methods, but found that only with Newton's method the computational efficiency was significantly improved. Only a few, detailed specialized studies mention the use of Newton's or similar methods to solve coupled balance schemes, (Collatz et al. , 1991; Pearcy et al., 1997; Soo-Hyung and Lieth , 2003; Dubois et al., 2007), or extensions of the photosynthesis-transpiration scheme along the leaf-plant-soil continuum in DGVMs (Bonan et al. , 2014) are mentioned, but none provide a documentation on the computational efficiency, or how the numerical method was implemented in the model and/or a code. In addition we test the effect of sensitive photosynthesis parameter on annual GPP of the computationally efficient model where we build on recent work by (Walker et al. , 2020).

We start with a short description of the different mathematical methods to find the zeros of a general nonlinear continuous function f and their advantages and disadvantages. Afterwards we introduce the relevant function f from the photosynthesis module and calculate its derivative. We then compare the performance of Newton's algorithm and bisection in terms of the number of iterations and the computational time that is necessary to achieve a given accuracy. Finally, we benchmark the updated LPJmL version to show that the simulated vegetation dynamics as well as storage and fluxes of carbon and water remain robust.

2 Solution of nonlinear equations

The computation of the ratio λ between intracellular and ambient CO_2 concentration requires to compute the zero of a function $f(\lambda)$. In most cases, this task cannot be solved analytically but requires a numerical approach, mostly based on iterative methods. Given a nonlinear continuous function $f : \mathbb{R} \to \mathbb{R}$, we want to find the zero(s) x_s of this function within a certain

interval $[a,b]$. While bisection, regula falsi and secant method are very simple to implement, Newton's method requires the computation of the derivative of f, which will be provided for the photosynthesis equation described in Sub-Section 3.2.
Here, the computational efficiency is determined by the speed of convergence. To compare the methods with respect to the speed of convergence we define the order of convergence: Let x_s be a zero of f found by computing a sequence (x_k) of approximate solutions via an iteration scheme. The iteration method has the order of convergence p if

$$\limsup_{k\to\infty} \frac{\|x_{k+1} - x_s\|}{\|x_k - x_s\|^p} = K \tag{1}$$

with $0 < K < \infty$ and $K < 1$ for $p = 1$. Thus a high order of convergence implies a fast convergence which on the other hand means fewer iteration steps. Numerically, the iteration is stopped either if the function value $f(x_k)$ of the iterate x_k is almost zero, i.e., less than a given accuracy y_{acc}, or if the iterate itself changes less than a given accuracy $|x_k - x_{k-1}| < x_{acc}$.
Let us introduce some of the methods in the following subsections, see Schwarz (2009) for details.

2.1 Bisection

For bisection we have to choose $[a,b]$ such that $f(a) \cdot f(b) < 0$, i.e. $f(a)$ and $f(b)$ have different signs. We compute the midpoint of the interval $x_m = \frac{a+b}{2}$ and its function value $f(x_m)$. If $|f(x_m)| < y_{acc}$ the search is complete, if not we check if $f(a) \cdot f(x_m) < 0$. If the latter is the case, x_s has to be in the interval $[a, x_m]$, otherwise in $[x_m, b]$. We repeat this bisection until either $|f(x_k)| < y_{acc}$ or $|x_k - x_{k-1}| < x_{acc}$. This method always converges but slowly with convergence order $p = 1$, i.e., linear convergence.

2.2 Regula falsi

For the regula falsi method, we also need to choose a, b such that $f(a) \cdot f(b) < 0$. Instead of the midpoint of $[a,b]$ we compute the next iterate x_1 for an approximation of x_s by computing the zero of the linear function through the points $(a|f(a))$ and $(b|f(b))$. Again we check if $|f(x_1)| < y_{acc}$ and abort or check if $f(a) \cdot f(x_1) < 0$ and repeat this procedure either with $[a, x_1]$ or $[x_1, b]$. Convergence is always assured and also linear, i.e., $p = 1$.

2.3 Secant method

The secant method only differs from the regula falsi in that the starting values $a = x_0$ and $b = x_1$ do not have to fulfill the condition $f(a) \cdot f(b) < 0$. The next iterate is computed by

$$x_{k+1} = x_k - f(x_k)\frac{x_k - x_{k-1}}{f(x_k) - f(x_{k-1})}. \tag{2}$$

This method can fail to converge depending on the starting values. If the method converges, it does so with order $p = 1,618$. Since the conditions on the starting values to ensure convergence depend on the knowledge of x_s, in practise a and b still have to fulfill the condition $f(a) \cdot f(b) < 0$.

2.4 Newton's method

Newton's method starts at an arbitrary approximation x_0 of x_s and uses the tangent of the function f at $(x_0, f(x_0))$ to compute the next iterate x_1 as the zero of the tangent. This is repeated, thus the next iterate is always computed from the previous one by

$$x_{k+1} = x_k - \frac{f(x_k)}{f'(x_k)}, \tag{3}$$

provided that $f'(x_k) \neq 0$. The method belongs to the class of fixed point iterations because the computation of the next iterate depends on the previous iterate only. If f is three times differentiable on $[a, b]$ and $f'(x_s) \neq 0$ then there exists an interval $I = [x_s - \delta, x_s + \delta]$ such that f is a contraction on I. It implies that for every start value from I, the method converges at least with order $p = 2$, (Schwarz, 2009). We remark that the gain in convergence speed has to be weighted against the time it takes to compute the derivative of f.

3 Application to the problem

We now analyse the difference in speed of convergence between the bisection and Newton's method when applied to the optimization equation of the photosynthesis routine of the LPJmL DGVM.

3.1 Definition of the function f

In presenting the function $f(\lambda)$, we follow the nomenclature of Schaphoff et al. (2018a), which contains a detailed description of the derivation of this function. A list of the used symbols is given in Appendix A. We want to find $\lambda = \frac{c_i}{c_a} = \frac{p_i}{p_a}$, i.e. the ratio between the intracellular and ambient CO_2 concentration, or partial pressure, resp., as the solution of the following equation

$$0 = f(\lambda) \quad = \quad A_{nd}(\lambda) + \left(1 - \frac{dayl}{24}\right) R_{leaf} - \frac{p_a(g_c - g_{min})}{1.6}(1 - \lambda). \tag{4}$$

Here A_{nd} the net daily photosynthesis, R_{leaf} the leaf respiration, $dayl$ the hours of daylight, p_a the ambient partial pressure, g_c the canopy conductance, and g_{min} the minimum canopy conductance for a specific plant functional type (PFT). The first term is the photosynthesis during daylight. It is the gross daily photosynthesis A_{gd} minus leaf respiration, $A_{nd}(\lambda) = A_{gd}(\lambda) - R_{leaf}$. The second term represents the dark respiration, i.e. respiration during night-time. The third term represents the photosynthesis that is possible to achieve a potential canopy conductance. In finding λ such that $f(\lambda) \approx 0$ we actually balance both light- and Rubisco-limited photosynthesis (first two terms) and photosynthesis related to the potential canopy conductance.
To shorten the formulas we define the abbreviation $C_{pg} = \frac{p_a(g_c - g_{min})}{1.6}$:

$$0 = f(\lambda) \quad = \quad A_{gd}(\lambda) - \frac{dayl}{24} R_{leaf} - C_{pg}(1 - \lambda). \tag{5}$$

The second summand does not depend on λ, whereas $A_{gd}(\lambda)$ has a more complex representation. The gross photosynthesis rate A_g is the minimum of the light-limited, J_C, and Rubisco-limited photosynthesis rate, J_E. It can be shown that the minimum

can be computed as

$$A_{gd}(\lambda) = \frac{dayl}{2\theta}\left[J_E(\lambda)+J_C(\lambda)-\sqrt{(J_E(\lambda)+J_C(\lambda))^2-4\theta J_E(\lambda)J_C(\lambda)}\right] \quad (6)$$

where θ is a shape parameter that allows for a gradual transition from one limitation to the other.

Light-limited photosynthesis depends on the absorbed photosythetically active radiation $APAR$, Rubisco-limited photosynthesis is determined by the maximum Rubisco capacity V_m:

$$J_E(\lambda) = C_1(\lambda)\frac{APAR}{dayl}, \quad (7)$$

$$J_C(\lambda) = C_2(\lambda)V_m. \quad (8)$$

Setting the internal partial pressure $p_i = \lambda p_a$ and using another abbreviation $C_K := K_c(1+\frac{[O_2]}{K_O})$, where K_c is the Michaelis constant for CO_2, $[O_2]$ and K_O are the partial pressure and the Michaelis constant for oxigen, we have

$$C_1(\lambda) = \begin{cases} T_{stress}\ \alpha_{C3}\ \frac{\lambda p_a-\Gamma_*}{\lambda p_a+(2)\Gamma_*} & \text{for C3- Photosynthesis} \\ T_{stress}\ \alpha_{C4}\ \frac{\lambda}{\lambda_{max_{C4}}} & \text{for C4- Photosynthesis} \end{cases} \quad (9)$$

$$C_2(\lambda) = \begin{cases} \frac{\lambda p_a-\Gamma_*}{\lambda p_a+C_K} & \text{for C3- Photosynthesis} \\ 1 & \text{for C4- Photosynthesis.} \end{cases} \quad (10)$$

Here, α_{C3} and α_{C4} are the intrinsic quantum efficiencies for CO_2 uptake in C_3 and C_4 plants, resp. Γ_* is the carbone dioxide compensation point and T_{stress} is a temperature stress function defined as

$$T_{stress} = \frac{1-0.01e^{T_3(T_d-T_4)}}{1+e^{T_1(T_2-T_d)}} \quad (11)$$

with T_d as the daily air temperature and T_1 to T_4 being PFT-specific temperature parameters, (Sitch et al., 2000). LPJmL simulates vegetation dynamics for the 10 PFTs; we provide the parameter values used for T_1 to T_4 in Appendix A, table A2, for the PFT types from Schaphoff et al. (2018a).

3.2 Derivative of f

To compute the derivative f' of f we rearrange (5):

$$f(\lambda) = A_{gd}(\lambda) + C_{pg}\lambda - C_{pg} - \frac{dayl}{24}R_{leaf} \quad (12)$$

Since the last two terms are constant the derivative is given by

$$f'(\lambda) = A'_{gd}(\lambda) + C_{pg}. \quad (13)$$

To determine A'_{gd} we apply sum, chain, and product rule of differentiation to (6) and get

$$A'_{gd}(\lambda) = \frac{dayl}{2\theta}\left[J'_E+J'_C-\frac{[J_E+J_C][J'_E+J'_C]-2\theta[J'_EJ_C+J_EJ'_C]}{\sqrt{(J_E+J_C)^2-4\theta J_EJ_C}}\right]. \quad (14)$$

The derivatives of J_E and J_C are given by

$$J'_E(\lambda) = C'_1(\lambda)\frac{APAR}{dayl}, \tag{15}$$

$$J'_C(\lambda) = C'_2(\lambda)V_m. \tag{16}$$

To compute C'_1 from (9) and C'_2 from (10) we use the quotient rule

$$C'_1(\lambda) = \begin{cases} T_{stress}\ \alpha_{C3}\ \frac{2(3)p_a\Gamma_*}{(\lambda p_a+(2)\Gamma_*)^2} & \text{for } C_3\text{- Photosynthesis} \\ \frac{T_{stress}\ \alpha_{C4}}{\lambda_{max_{C4}}} & \text{for } C_4\text{- Photosynthesis} \end{cases} \tag{17}$$

$$C'_2(\lambda) = \begin{cases} \frac{p_a(C_K+\Gamma_*)}{(\lambda p_a+C_K)^2} & \text{for } C_3\text{- Photosynthesis} \\ 0 & \text{for } C_4\text{- Photosynthesis.} \end{cases} \tag{18}$$

We describe the consequent changes in the model code which were required to implement the computation of the derivative *fcnd*(λ) in the Appendix B.

The function f is defined for all $\lambda > 0$, as long as $(J_E(\lambda)+J_C(\lambda))^2 \geq 4\theta J_E(\lambda)J_C(\lambda)$. As a composition of at least three times differentiable functions it fulfills the differentiability condition of Newton's method. The parameters in the definition of f vary with the geographic location and season. A plot of f for parameters from different locations (boreal, temperate, and tropical) and at different times can be seen in Figure 1.

The condition $f'(\lambda) \neq 0$ as well as the suitability of a staring value can not be generally ensured. In all our computations convergence was not a problem. To be on the safe side, one can implement a hybrid method that switches to bisection if convergence of the iterates does not occur.

4 Numerical performance and discussion

We have tested the different methods in the routine regarding computational time and number of iterations for given accuracy x_{acc}. There was no significant speed-up with the secant and regula falsi method. Hence, we concentrated on the comparison of Bisection and Newton's method and describe the outcome in this section.

In a first test, the LPJmL model was run over 120 simulation years and the number of iterations in the Bisection and Newton's routine was counted and averaged over all grid cells and one year (Figure 2). For $x_{acc} = 0.01$ this number was about 3 for Newton's method and 7 for Bisection (dotted lines in Figure 2). When x_{acc} was set to 0.001 the number of iterations with Newton's method increased only slightly whereas the Bisection method needed 9 to 10 iterations (solid lines in Figure 2). Until now, the bisection algorithm used 10 as the maximal number of iterations. Using maximum 10 iterations fits to the interval width of $2^{-10} \approx 0.001$, our accuracy measure x_{acc}. Increasing the maximum number of iterations had no effect on the number of required iterations. We conclude that Newton's method reduces the necessary number of iteration to a third.

In a next step, a spin-up run of LPJmL over 5000 simulation years was conducted to compare the time performance using both routines. Usually, LPJmL simulation experiments start from bare ground, i.e. initial vegetation conditions are not prescribed. Therefore, a spin-up run is used to bring all vegetation and soil carbon pools into equilibrium with climate. For the usually

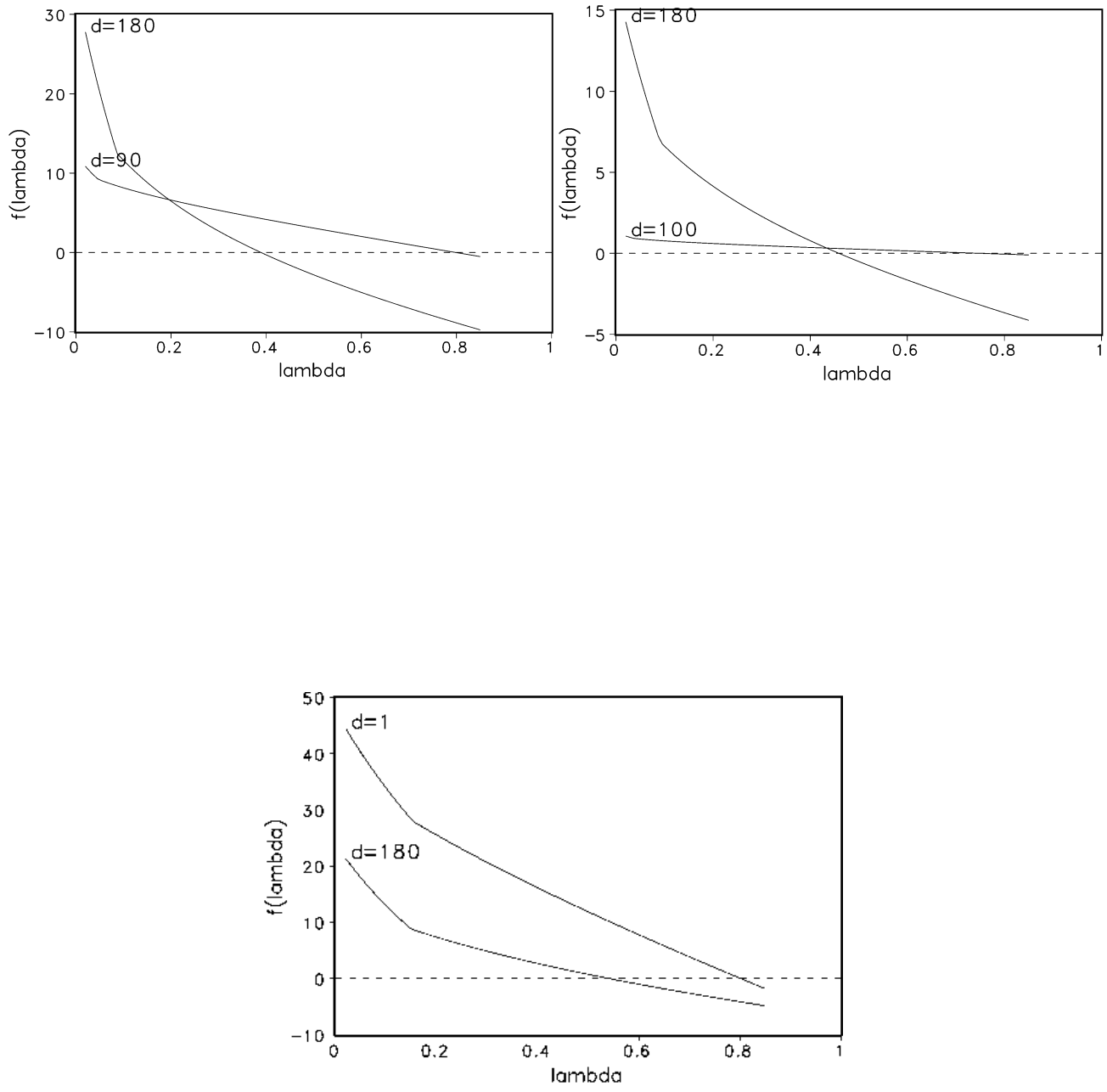

Figure 1. Function $f(\lambda)$ for a set of parameters from different days in 1901 and locations, namely Hainich (Germany, mixed-temperate forest; upper left), Seiteminen (Finland, boreal forest; upper right) and Santarem (Brazil, tropical rainforest; lower). d denotes the day in year 1901.

implemented accuracy $x_{acc} = 0.1$ the computation time for 5000 years was about 5250 s in both cases. This means that the advantage of Newton's method in terms of iteration numbers is levelled by the additional time for computing the derivative of f. For $x_{acc} = 0.01$, the Bisection method needed 6700 s, while Newton's method 5600 s. Thus a reduction of about 16% in time could be observed. It implies that with almost the same amount of time (5250 s vs. 5600 s) a higher accuracy can be achieved with Newton's method (Figure 3). While the accuracy y_{acc} does not increase significantly for the Bisection method for $x_{acc} = 0.001$, we gain 2 orders of magnitude increase in y_{acc} for the Newton's method. As a result, a change of x_{acc} from 0.1 to 0.01 will be permanently implemented in the LPJmL model for future model applications. We expect that with the implementation of new model developments that affect the photosynthesis module (e.g., nutrient limitation from nitrogen and leaf temperatures) an efficient and increased model accuracy (y_{acc}) for finding the zero of $f(\lambda)$ will be even more important. It can be expected that the computation time for the Bisection method would increase substantially, while increasing only moderately for Newton's method.

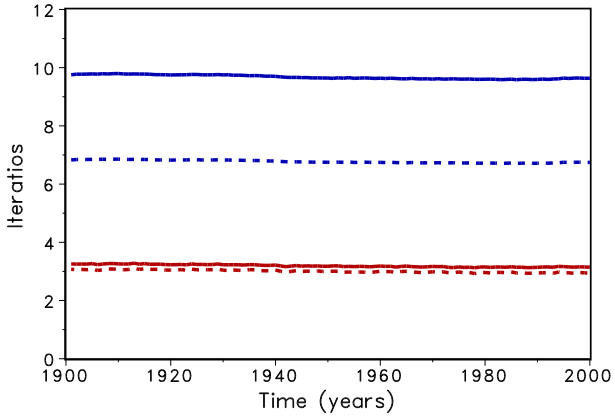

Figure 2. Average number of iteration for Bisection (upper lines, blue) and Newton (lower lines, red) for accuracy $x_{acc} = 0.01$ (dotted) and 0.001 (solid)

In order to check if the implementation of Newton's method is robust for all important model variables, we performed a transient simulation with the LPJmL model starting from the spin-up and covering the years 1901-2000. Model configuration and input data are as in Schaphoff et al. (2018a). We compared the main diagnostic variables of the published LPJmL4.0 version against the version using the Newton's Method (see Appendix C). We found that most global diagnostic variables related to fluxes and storage of carbon and water had differences of $< \pm 1.0\%$, including total vegetated area. Only marginal changes (+3 gC per mA^2 and month) in net primary productivity (NPP), heterotrophic respiration and evaporation are seen mainly in Europe and southern as well as southeastern Asia. The reductions in carbon storage in litter and soil are very small and apply only to the boreal zone across the northern hemisphere and central Europe (compare spatial maps of carbon and water variables in Appendix C).

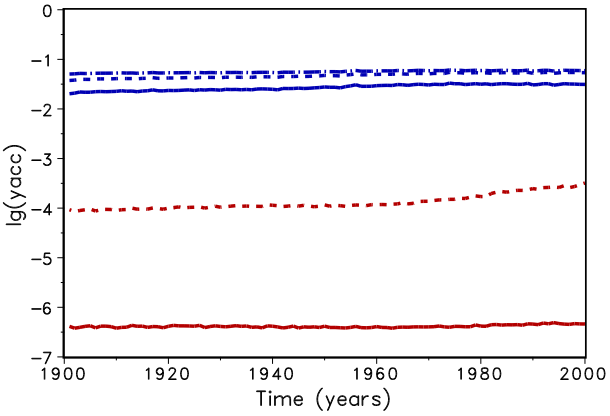

Figure 3. Mean decadic logarithm of the accuracy y_{acc} for Bisection (upper lines, blue) and Newton (lower lines, red) for accuracy $x_{acc} = 0.01$ (dotted) and 0.001 (solid). The dashed-dotted line shows the accuracy of the original version of LPJmL.

The photosynthesis module is also applied to the crop functional types and managed grassland within LPJmL4.0. Therefore, sawing dates, crop productivity and harvest are among the simulated variables. Comparing both model versions in the model benchmark, we found that global harvest changed for a number of crops. Rainfed and irrigated rice increased by 5% and 8%, respectively, mainly in India and southeast Asia. Harvest of rainfed temperate cereals increased by $< 1.0\%$, mainly found in central Europe. Harvest of irrigated temperate cereals (incl. wheat) increased by 4.5%, which mainly applied to India as well. Harvest of irrigated and rainfed soybean increased by 2.3% and 1.5% globally, the differences are mainly found in the US and Brazil. All other crop functional types had marginal to zero changes in global productivity as well as simulated harvest (see Table in Appendix C).

For all global carbon pools (vegetation and soil) and carbon (GPP, heterotrophic respiration and fire emissions) as well as water fluxes (transpiration and runoff) we found no difference in the temporal changes in the transient simulation over the 20th century. All variables showed similar, if not identical dynamics (data not shown). Small changes were found in the fractional coverage of plant functional types, i.e. most differences were negligible. The fractional coverage of Temperate broadleaved summergreen trees increased by 4.8% globally, which mainly applies to Europe, northeastern US and parts of China. Increases in temperate C_3 grasses are found in the boreal zone, summing up to 4.8% globally. Marginal changes of $< 0.5\%$ per grid cell are found for all other PFTs which imply small adjustments in vegetation composition in these vegetation zones (see difference maps in Appendix C). Comparisons using flux tower measurements on carbon and water fluxes as well as discharge data showed no differences so that we can conclude that also for these variables the results are robust (data not shown). We can therefore conclude that the LPJmL results were robust before, but are now achieved due to improved accuracy of the photosynthesis routine.

In addition to improving the computational efficiency and numerical precision, parameter uncertainties have been tested following Walker et al. (2020), who tested the sensitivity of $\theta, \alpha_{C3}, b_{C3}, k_{c25}, K_{o25}$ on their impacts on global GPP. The LPJmL model computes V_m as follows Schaphoff et al. (2018a), eq. (35):

$$V_m = \frac{1}{b_{C3}} \cdot \frac{c_1}{c_2} \cdot ((2\theta - 1) * s - (2\theta * s - c_2) * \sigma) \cdot APAR. \quad (19)$$

Therefore, the sensitivity of V_{cmax} results from varying b_{C3} indirectly since the reciprocal of b_{C3} is used to calculate V_{cmax} in a linear equation. Varying b_{C3} is therefore the adequate sensitivity test which relates to V_{cmax}. We varied each parameter by 10% independently and find that θ ($\alpha_{C3}, b_{C3}, k_{c25}, K_{o25}$) increases global annual GPP (AGPP, hereafter) by 1.67% (+6.69%, -1.67%, -0.35%, +0.14%). Table 1 shows the difference of the two most important parameter on global AGPP.

parameter	Δ GPP relative in $\%$	Δ GPP absolute (GtC/yr)
θ	1.67	2.384
α_{C3}	6.68	9.542
b_{C3}	-0.56	-0.798
k_{c25}	-0.35	-0.506
K_{o25}	0.14	0.199

Table 1.

Change in the AGPP after varying the listed parameters by 10%. GPP is calculated as the global average mean for the years 1901-2000.

Geographically, increasing θ yields higher AGPP mainly in the tropics and temperate forest regions, where AGPP increases up to 100 gC/m^2. However, AGPP increases between 200 and 500 gC/m^2 when changing α_{C3}, see Fig.4. It turns out that AGPP is increased in all regions, where LPJmL simulates woody PFTs. Also here, largest effects are seen in (sub-)tropical and temperate regions which span larger areas than the areas with increased AGPP as a result of varying θ.

We remark that future work on the photosynthesis approach could focus on the new Johnson and Berry scheme (Johnson and Berry , 2021) with the advantage of calculating gas-exchange and relying less on empirical coefficients.

5 Conclusions

The computational load of Dynamic Global Vegetation Models, caused by increased complexity of the modelling processes, has been so far counteracted by the used high performance computing systems. However, more recently it has become clear that updates in computing infrastructure are not sufficient anymore. Consequently, we proposed to carefully evaluate the algorithmic structure of DGVMs and identify and update routines that can benefit from the use of modern mathematical methods. As a showcase, we investigated the photosynthesis model in the LPJmL DGVM. Specifically, we investigated the computation of the ratio λ between intracellular and ambient CO_2, which is obtained as the zero of a function f. We proposed to replace the so far used bisection method by a Newton method, which is known to converge significantly faster. We carefully compared

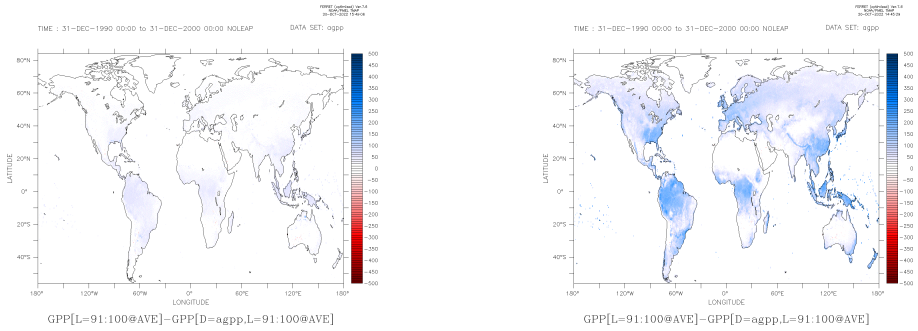

Figure 4. Parameter sensitivity on Annual Gross Primary Productivity (AGPP, average of 1901-2000) shown as difference between new parameter and reference simulation. Both simulations have the Newton approach implemented. Increasing θ by 10 % increased AGPP mainly in forested regions (left panel). Increasing α_{C3} by 10 % has a much larger effect on AGPP, especially in the tropics (right panel).

the model performance of the published LPJmL4.0 version with the version developed in this study and found that the model performance is robust. Using a more sophisticated mathematical method in the photosynthesis module allowed for a higher precision in the computation of λ and resulted in slightly increased productivity in continental and mountainous areas. We think that the new results are more accurate than the previous version due to the higher accuracy of the Newton method visible in Figure 3. With the currently implemented accuracy bounds, the run-time of the model with the Newton routine implemented is about 16% lower than the old version. This advantage will be much more prominent if the complexity of the model is further extended or if more accurate modelling results are required. Consequently, the Newton based routine will be implemented in the LPJmL model. Additionally we believe that the Newton method can also be applied to photosynthesis modules in other DGVMs and increase model accuracy and/or computational efficiency.

Code and data availability. The model code is available at https://doi.org/10.5281/zenodo.6644541 .

Appendix A: Parameters in photosynthesis

A_{nd}	daily net photosynthesis
dayl	day length
R_{leaf}	leaf respiration
p_a	ambient partial pressure
g_c	canopy conductance
g_{min}	PFT-specific minimum canopy conductance
A_{gd}	daily gross photosynthesis
θ	co-limitation (shape) parameter
J_E	light limited photosynthesis rate
J_C	Rubisco limited photosynthesis rate
APAR	absorbed photosynthetically active radiation
V_m	maximum Rubisco capacity
K_C	Michaelis constant for CO_2
$[O_2]$	O_2 partial pressure
K_O	Michaelis constant for O_2
T_{stress}	Temperature stress function limiting photosynthesis at low and high temperatures
α_{C3}	intrinsic quantum efficiencies for CO_2 uptake in C_3 plants
α_{C4}	intrinsic quantum efficiencies for CO_2 uptake in C_4 plants
Γ_*	carbone dioxide compensation point
λ_{maxC4}	maximum ratio of intracellular to ambient CO_2 for C_4-photosynthesis

Table A1.

General parameters used in the photosynthesis routine. PFT - Plant functional type

Plant Functional Type (PFT)	T_1	T_2	T_3	T_4
Tropical broadleaved evergreen tree	2.0	25.0	30.0	55.0
Tropical broadleaved raingreen tree	2.0	25.0	30.0	55.0
Temperate needleleaved evergreen tree	-4.0	20.0	30.0	42.0
Temperate broadleaved evergreen tree	-4.0	20.0	30.0	42.0
Temperate broad-leaved summergreen tree	-4.0	20.0	25.0	38.0
Boreal needle-leaved evergreen tree	-4.0	15.0	25.0	38.0
Boreal needle-leaved summergreen tree	-4.0	15.0	25.0	38.0
Polar C_3 grass	-4.0	10.0	30.0	45.0
Temperate C_3 grass	-4.0	10.0	30.0	45.0
Tropical C_4 grass	6.0	20.0	45.0	55.0

Table A2.

PFT-specific parameter for temperature stress function (eq.12) in °C. PFT types as in Schaphoff et al. (2018a)

Appendix B: Programming

To implement Newton's method in the LPJmL code, changes had to be made in the functions `photosynthesis.c`, `gp_sum.c` and `water_stressed.c`. (separate file)

New function `newton.c`: see source code in a separate file.

Remark

The function `photosynthesis.c` within LPJmL computes the value $A_{nd}(\lambda) + \left(1 - \frac{dayl}{24}\right) R_{leaf}$ for a given λ. In the function `water_stressed.c` the function `fcn`(λ) is defined as $fcn(\lambda) = C_{pg} * (1 - \lambda) - photosythesis(lambda)$, i.e. $fcn = -f$. In order to use Newton's Method we have to compute not only *fcn*(λ) but also its derivative $fcnd(\lambda) = -f'(\lambda)$.

Appendix C: Benchmark results

LPJmL Benchmark

Actual vegetation

Author: Werner von Bloh

Date: 27.04.2022

Benchmark run: newton_e3/output/

Run: bisect_e3/output/

Description: LPJ Benchmark 2022-04-27

Global sums: Veg. incl. LU 1991-2000

Parameter	Lit. estimates	Bm. Run	Run	Diff. abs.	Diff %
Vegetation carbon [GtC]	460 - 660 (1, 2, 3)	595.9	596.2	0.231	0.039
Total soil carbon density [GtC]	2376 - 2456 (4), 1567 (5), 1395 (6)	1862	1862	-0.08	-0.004
Litter carbon [GtC]	NA	151.3	151.4	0.116	0.077
Fire carbon emission [GtC/year]	2.14 (1.6 Nat.Fire) (7, 8, 9, 10)	3.108	3.109	0.001	0.036
Establishment flux [GtC/year]	NA	0.161	0.161	0	-0.002
Area All natural vegetation [M ha]	NA	7767	7767	-0.119	-0.002
Area Tropical broadleaved evergreen tree [M ha]	NA	1180	1179	-0.237	-0.02
Area Tropical broadleaved raingreen tree [M ha]	NA	1280	1280	0.448	0.035
Area Temperate needleleaved evergreen tree [M ha]	NA	364	360.8	-3.166	-0.87
Area Temperate broadleaved evergreen tree [M ha]	NA	322	321.5	-0.467	-0.145
Area Temperate broadleaved summergreen tree [M ha]	NA	136	142.5	6.517	4.792
Area Boreal needleleaved evergreen tree [M ha]	NA	429.2	426.8	-2.393	-0.558
Area Boreal broadleaved summergreen tree [M ha]	NA	916.8	919.6	2.814	0.307

Parameter	Lit. estimates	Bm. Run	Run	Diff. abs.	Diff %
Area Boreal needleleaved summergreen tree [M ha]	NA	378.3	380.7	2.398	0.634
Area Tropical c4 grass [M ha]	NA	893.2	890.6	-2.573	-0.288
Area Temperate c3 grass [M ha]	NA	535.7	545.2	9.472	1.768
Area Polar c3 grass [M ha]	NA	1332	1320	-12.93	-0.971
NPP [GtC/year]	66.05 (11), 62.6 (2), 49.52 - 59.74 (12)	62.81	62.87	0.064	0.102
Heterotrophic respiration [GtC/year]	NA	50.78	50.83	0.044	0.086
Evaporation [10.. km3/year]	NA	9.644	9.661	0.017	0.173
Transpiration [10.. km3/year]	NA	47.83	47.82	-0.011	-0.024
Interception [10.. km3/year]	NA	7.914	7.912	-0.002	-0.024
Runoff [10.. km3/year]	NA	54.3	54.23	-0.064	-0.118
Harvested carbon rainfed tece [Mt DM/year]	524.08 (13)	458.5	462.6	4.106	0.895
Harvested carbon rainfed rice [Mt DM/year]	492.66 (13)	125.2	131.5	6.304	5.035
Harvested carbon rainfed maize [Mt DM/year]	498.33 (13)	434.9	434.8	-0.07	-0.016
Harvested carbon rainfed soybean [Mt DM/year]	NA	126.3	128.1	1.87	1.481
Harvested carbon irrigated tece [Mt DM/year]	524.08 (13)	156.7	163.7	7.038	4.493
Harvested carbon irrigated rice [Mt DM/year]	492.66 (13)	206.4	223	16.64	8.062
Harvested carbon irrigated maize [Mt DM/year]	498.33 (13)	153.1	153.1	-0.002	-0.001
Harvested carbon irrigated soybean [Mt DM/year]	NA	12.03	12.3	0.268	2.229
tree cover fraction [-]	NA	0.644	0.645	0.001	0.12

(1) Olson et al. 1985, (2) Saugier et al. 2001, (3) WBGU 1998, (4) Batjes et al. 1996, (5) Eswaran et al. 1993, (6) Post et al. 1982, (7) Seiler & Crutzen 1980, (8) Andreae & Merlet 2001, (9) Ito & Penner 2004, (10) van der Werf et al. 2004, (11) Vitousek et al. 1986, (12) Ramakrishna et al. 2003, (13) FAOSTAT 1990-2000

Table D1. Global numbers for benchmark with bisection and newton method

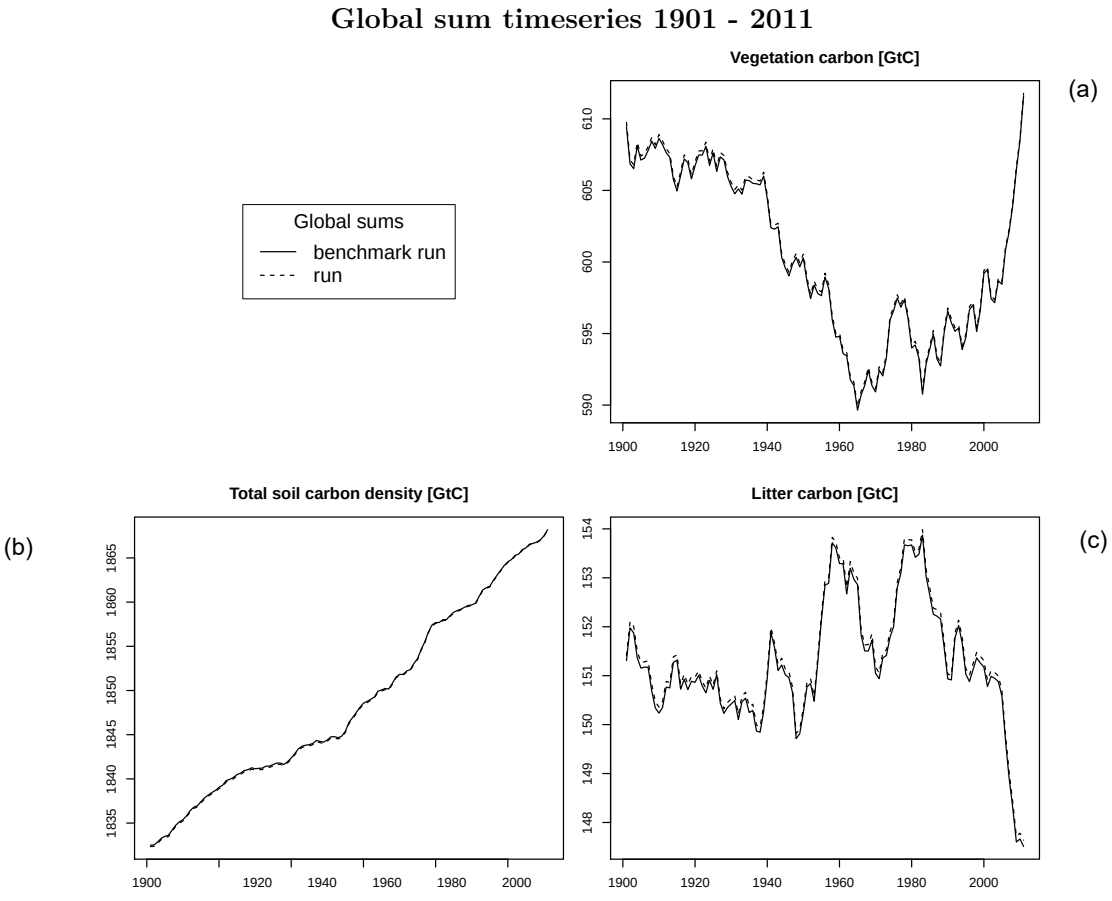

Figure D1. Global numbers for (a) vegetation carbon, (b) total soil carbon,(c) litter carbon

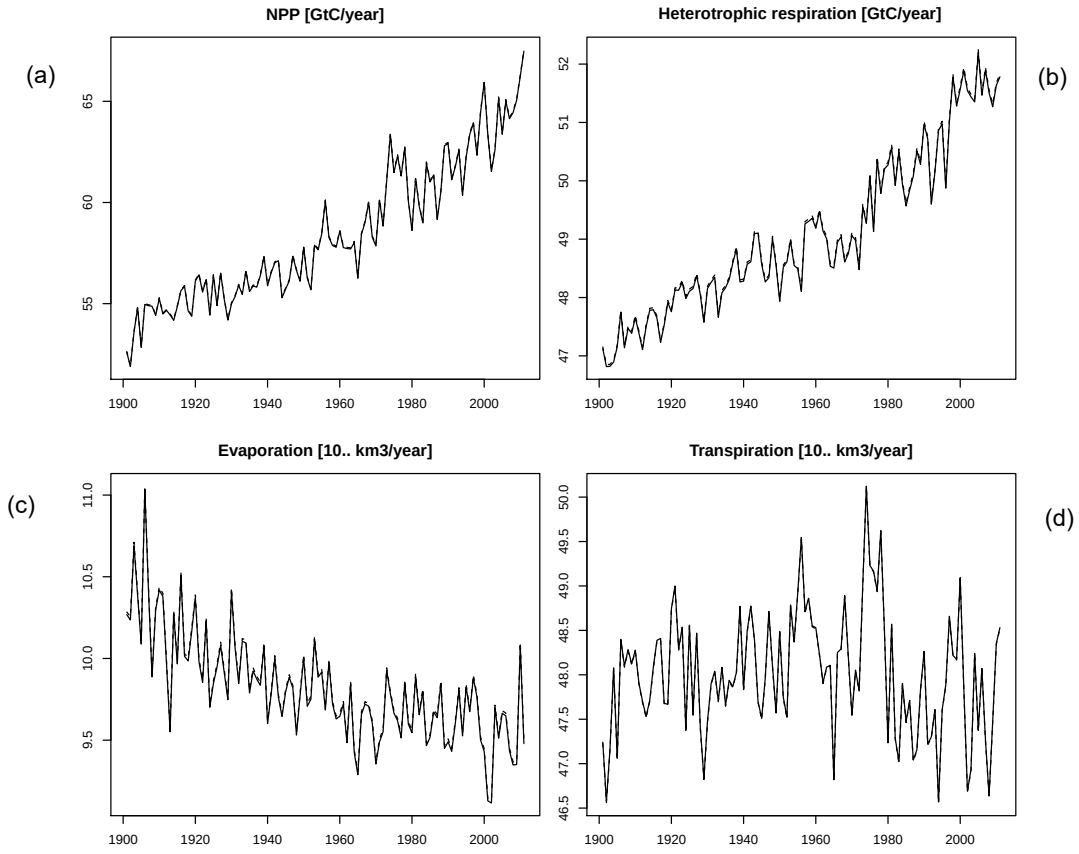

Figure D2. Global sum for time series of (a) NPP, (b) heterotrophic respiration, (c) evaporation, (d) transpiration.

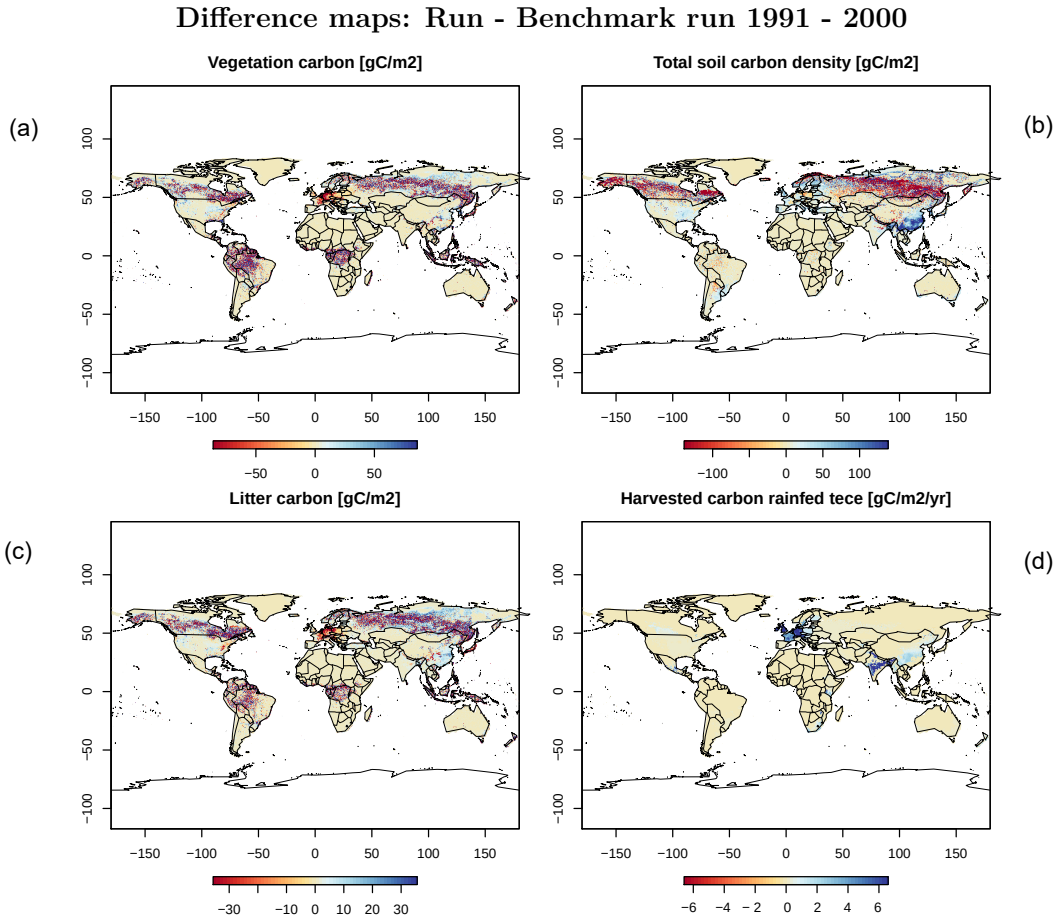

Figure D3. Difference maps of (a) vegetation carbon, (b) soil carbon, (c) litter carbon, (d) harvested carbon of rainfed temperate cereals (tece).

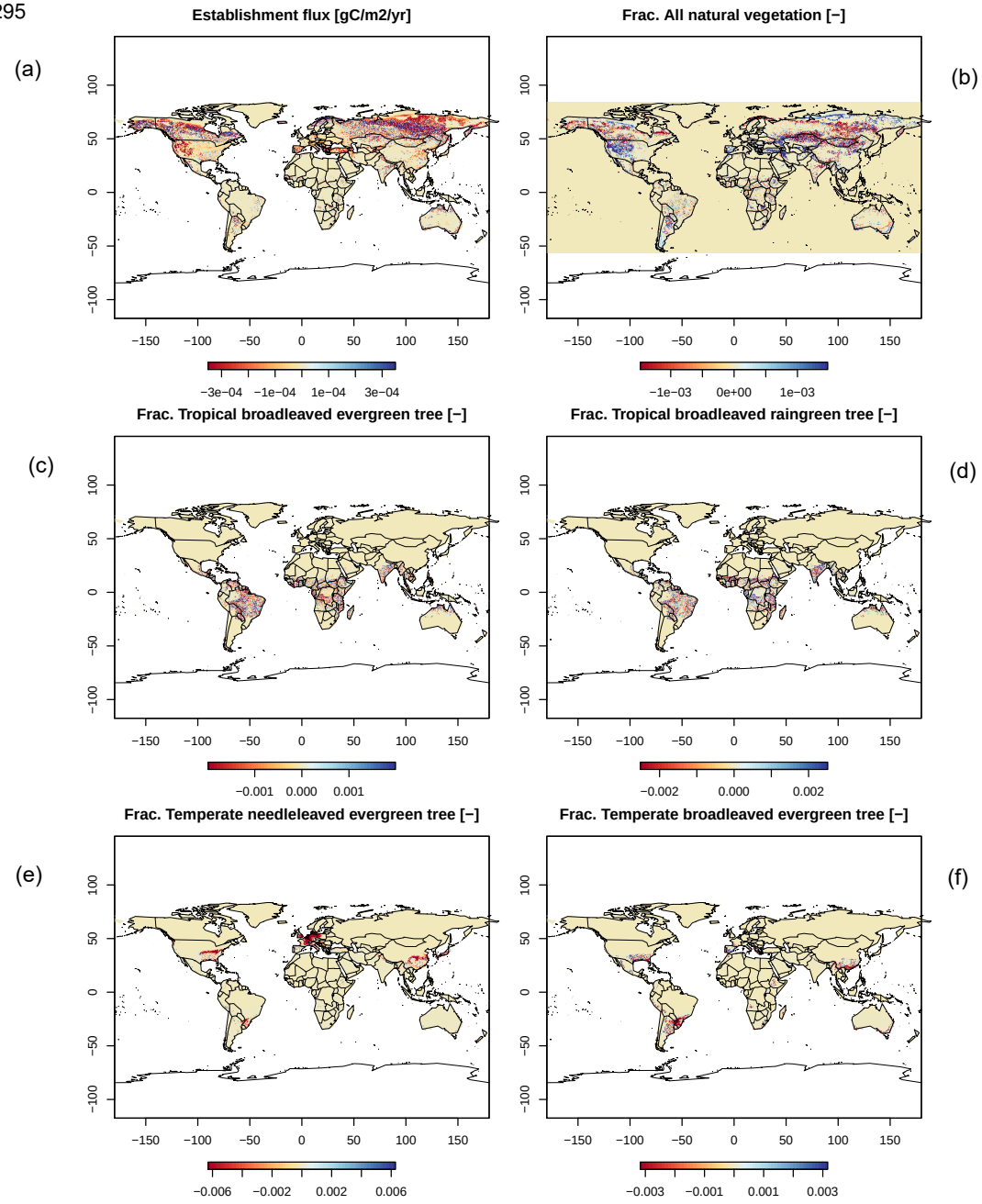

Figure D4. Difference maps of (a) establishment, (b) all natural vegetation, (c) frac. tropical broadleaved evergreen, (d) frac. tropical broadleaved raingreen, (e) frac. temperate needleleaved evergreen, (f) frac. temperate broadleaved evergreen.

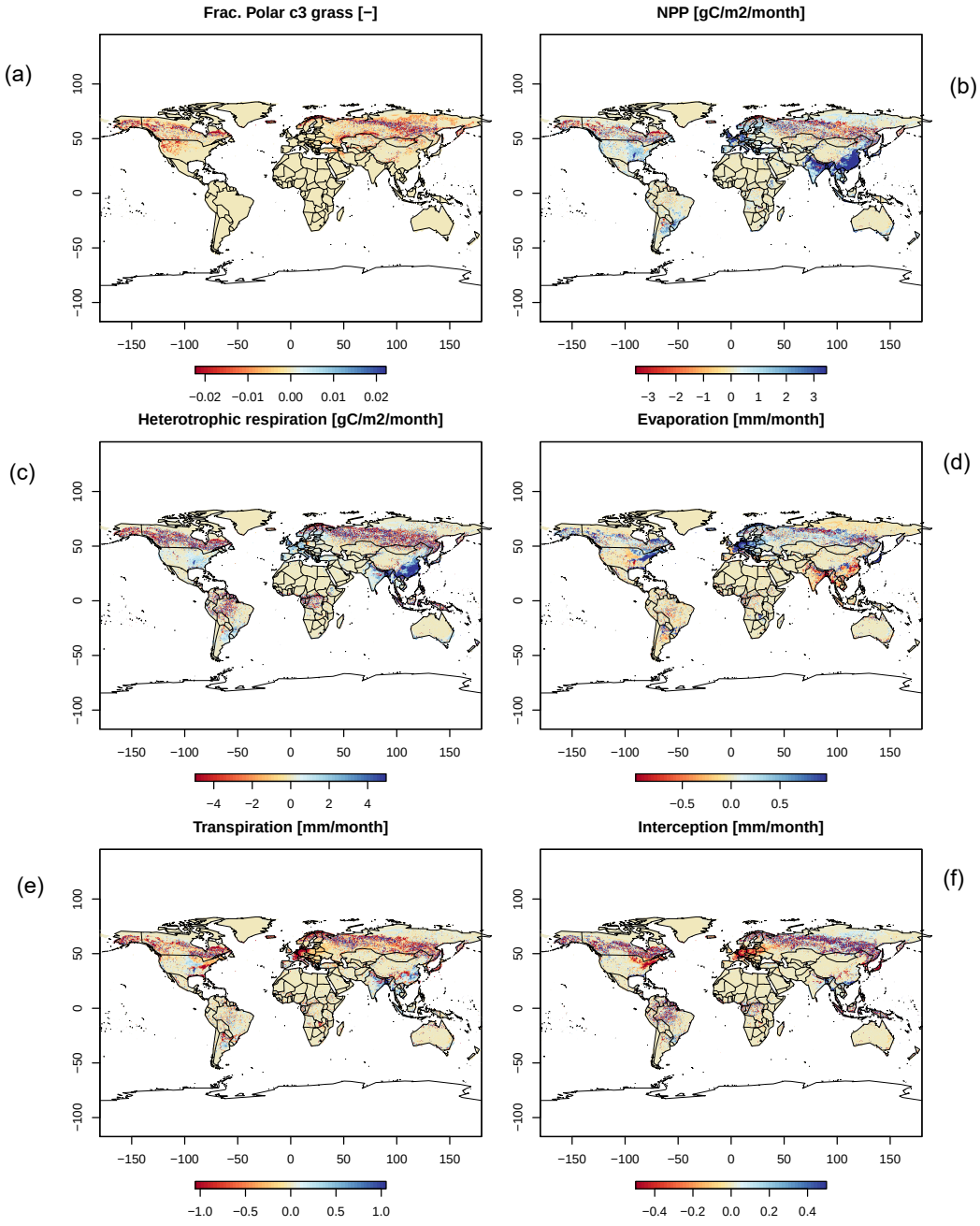

Figure D5. Difference maps of (a) frac. polar C3 grass, (b) NPP, (c) heterotrophic respiration, (d) evaporation, (e) transpiration, (f) interception.

(a)

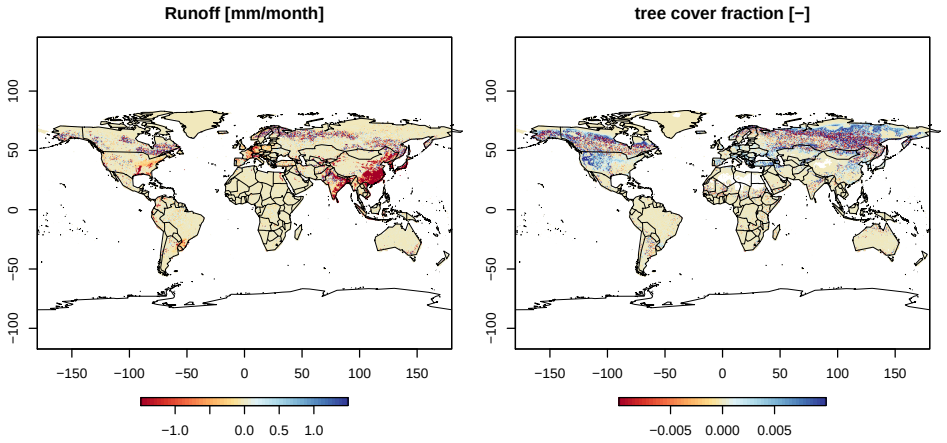

(b)

Figure D6. Difference maps of (a) runoff and (b) tree cover fraction.

Author contributions. JN and RR performed the mathematical analysis, JN and WvB implemented and tested the new numerical methods, WvB conducted the simulation experiments and analysed the model performance and computation efficiency. JN and KT wrote the paper, all authors contributed to the writing of the paper and discussion of the model study throughout to develop the work.

Competing interests. There are no competing interests.

Acknowledgements. The authors gratefully acknowledge the European Regional Development Fund (ERDF), the German Federal Ministry of Education and Research, and the Land Brandenburg for supporting this project by providing resources on the high-performance computer system at the Potsdam Institute for Climate Impact Research. We thank Marie Hemmen from PIK for her support in benchmarking the LPJmL model.

References

Bonan, G.B.: Land–atmosphere CO2 exchange simulated by a land surface process model coupled to an atmospheric general circulation model. Journal of Geophysical Research, 100, 2817–2831, 1995.

Bonan, G. B., Williams, M., Fisher, R. A., and Oleson, K. W.: Modeling stomatal conductance in the earth system: linking leaf water-use efficiency and water transport along the soil–plant–atmosphere continuum, Geosci. Model Dev., 7, 2193–2222, https://doi.org/10.5194/gmd-7-2193-2014, 2014.

Collatz, G.J., Ball, J.T., Grivet, C. and Berry, J.A.: Physiological and environmental regulation of stomatal conductance, photosynthesis and transpiration: a model that includes a laminar boundary layer. Agric. For. Meteorol,, 54: 107-136, https://doi.org/10.1016/0168-1923(91)90002-8, 1991.

Collatz G.J., Ribas-Carbo M., Berry J.A.: Coupled Photosynthesis-Stomatal Conductance Model for Leaves of C4 Plants. Functional Plant Biology 19, 519-538, https://doi.org/10.1071/PP9920519, 1992.

Cox P.M., Huntingford C., and Harding R.J.: A canopy conductance and photosynthesis model for use in a GCM land surface scheme. Journal of Hydrology 212–213, 79–94, 1998.

De Kauwe, M. G., Kala, J., Lin, Y.-S., Pitman, A. J., Medlyn, B. E., Duursma, R. A., Abramowitz, G., Wang, Y.-P., and Miralles, D. G.: A test of an optimal stomatal conductance scheme within the CABLE land surface model, Geosci. Model Dev., 8, 431–452, https://doi.org/10.5194/gmd-8-431-2015, 2015.

Dubois, J.-J.B., Fiscus, E.L., Booker, F.L., Flowers, M.D. and Reid, C.D.: Optimizing the statistical estimation of the parameters of the Farquhar–von Caemmerer–Berry model of photosynthesis. New Phytologist, 176, 402-414, https://doi.org/10.1111/j.1469-8137.2007.02182.x, 2007

Dufresne, J.L., Foujols, M.A., and Denvil, S. et al.: Climate change projections using the IPSL-CM5 Earth System Model: from CMIP3 to CMIP5. Clim Dyn 40, 2123–2165, https://doi.org/10.1007/s00382-012-1636-1, 2013.

Farquhar, G. D., von Caemmerer, S., and Berry, J. A.: A biochemical model of photosynthetic CO2 assimilation in leaves of C3 species. Planta, 149(1), 78–90, https://doi.org/10.1007/BF003 86231, 1980.

Haxeltine, A., and Prentice, I. C.: BIOME3: An equilibrium terrestrial biosphere model based on ecophysiological constraints, resource availability, and competition among plant functional types, Global Biogeochemical Cycles, 10, 693-709, https://doi.org/10.1029/96GB023441996, 1996.

Haxeltine, A., and Prentice, I. C.: A general model for the light-use efficiency of primary production, Functional Ecology, 10, 551-561, https://doi.org/10.2307/2390165, 1996.

Johnson, J.E. and Berry, J.A.: The role of cytochrome b6f in the control of steady- state photosynthesis: a conceptual and quantitative model, Photosynthesis Research, 148(3), pp.101-136, 2021

Knauer, J., Werner, C., and Zaehle, S.: Evaluating stomatal models and their atmospheric drought response in a land surface scheme: A multibiome analysis, J. Geophys. Res. Biogeosci., 120, 1894– 1911, doi:10.1002/2015JG003114, 2015.

Krinner, G., Viovy, N., Noblet-Ducoudré, N. d., Ogée, J., Polcher, J., Friedlingstein, P., Ciais, P., Sitch, S., and Prentice, I. C.: A dynamic global vegetation model for studies of the coupled atmosphere-biosphere system, Global Biogeochemical Cycles, 19, https://doi.org/10.1029/2003GB002199, 2005.

Masson-Delmotte, V., Zhai, P., Pirani, A., Connors, S.L., Péan, C., Berger, S., Caud, N., Chen, Y., Goldfarb, L., Gomis, M.I., Huang, M., Leitzell, K., Lonnoy, E., Matthews, J.B.R., Maycock, T.K., Waterfield, T., Yelekçi, O., Yu, R., and Zhou, B., (eds.) IPCC, 2021: Summary

for Policymakers. In: Climate Change 2021: The Physical Science Basis. Contribution of Working Group I to the Sixth Assessment Report of the Intergovernmental Panel on Climate Change, Cambridge University Press. In Press. https://doi.org/10.1017/9781009157896.

Oleson, K. W., Lawrence, D. M., Bonan, G. B., Drewniak, B., Huang, M., Koven, C. D., Levis, S., Li, F., Riley, W. J., Subin, Z. M., Swenson, S. C., Thornton, P. E., Bozbiyik, A., Fisher, R., Heald, C. L., Kluzek, E., Lamarque, J.-F., Lawrence, P. J., Leung, L. R., Lipscomb, W., Muszala, S., Ricciuto, D. M., Sacks, W., Sun, Y., Tang, J., and Yang, Z.-L.: Technical description of version 4.5 of the Community Land Model (CLM), NCAR Tech. Note NCAR/TN-503+STR, National Center for Atmospheric Research, Boulder, Colorado, 420 pp., 2013.

Oliver, R. J., Mercado, L. M., Clark, D. B., Huntingford, C., Taylor, C. M., Vidale, P. L., McGuire, P. C., Todt, M., Folwell, S., Shamsudheen Semeena, V., and Medlyn, B. E.: Improved representation of plant physiology in the JULES-vn5.6 land surface model: photosynthesis, stomatal conductance and thermal acclimation, Geosci. Model Dev., 15, 5567–5592, https://doi.org/10.5194/gmd-15-5567-2022, 2022.

O'Neill, B. C., Tebaldi, C., van Vuuren, D. P., Eyring, V., Friedlingstein, P., Hurtt, G., Knutti, R., Kriegler, E., Lamarque, J.-F., Lowe, J., Meehl, G. A., Moss, R., Riahi, K., and Sanderson, B. M.: The Scenario Model Intercomparison Project (ScenarioMIP) for CMIP6, Geoscientific Model Development, 9, 3461–3482, https://doi.org/10.5194/gmd-9-3461-2016, 2016.

Pearcy, R.W., Gross, L.J. and HE, D.: An improved dynamic model of photosynthesis for estimation of carbon gain in sunfleck light regimes. Plant, Cell and Environment, 20: 411-424. https://doi.org/10.1046/j.1365-3040.1997.d01-88.x, 1997.

Pitman, A.J.: The evolution of, and revolution in, land surface schemes designed for climate models. Int. J. Climatol., 23, 479-510, https://doi.org/10.1002/joc.893, 2003.

Pörtner, H.-O., Roberts, D.C., Poloczanska, E.S., Mintenbeck, K., Tignor, M., Alegria, A., Craig, M., Langsdorf, S., Löschke, S., Möller, V., Okem, A. (eds.) IPCC, 2022: Summary for Policymakers In: Climate Change 2022: Impacts, Adaptation, and Vulnerability. Contribution of Working Group II to the Sixth Assessment Report of the Intergovernmental Panel on Climate Change, Cambridge University Press. In Press.

Prentice, I. C., Bondeau, A., Cramer, W., Harrison, S. P., Hickler, T., Lucht, W., Sitch, S., Smith, B., and Sykes, M. T.: Dynamic global vegetation modelling: quantifying terrestrial ecosystem responses to large-scale environmental change. In: Canadell, J.G., Pataki, D. E., and Pitelka L. F. (Eds.),Terrestrial Ecosystems in a Changing World, Springer, Springer Nature, https://doi.org/10.1007/978-3-540-32730-1, 2007.

Reichstein, M., Camps-Valls, G., Stevens, B., Jung, M., Denzler, J., Carvalhais, N., and Prabhat: Deep learning and process understanding for data-driven Earth system science, Nature, 566, 195-204, https://doi.org/10.1038/s41586-019-0912-1, 2019.

Reick, C., Raddatz, T., Brovkin, V., and Gayler, V.: Representation of natural and anthropogenic land cover change in MPI-ESM, J. Adv. Model. Earth Syst., 5, 459–482, doi:10.1002/jame.20022, 2013.

Schaphoff, S., von Bloh, W., Rammig, A., Thonicke, K., Biemans, H., Forkel, M., Gerten, D., Heinke, J., Jägermeyr, J., Knauer, J., Langerwisch, F., Lucht, W., Müller, C., Rolinski, S., and Waha, K.: LPJmL4 - a dynamic global vegetation model with managed land, Part 1: Model description, Geoscientific Model Development, 11, 1343-1375, https://doi.org/10.5194/gmd-11-1377-2018, 2018.

Schaphoff, S., Forkel, M., Müller, C., Knauer, J., von Bloh, W., Gerten, D., Jägermeyr, J., Lucht, W., Rammig, A., Thonicke, K., and Waha, K.: LPJmL4 - A dynamic global vegetation model with managed land, Part 2: Model evaluation, Geoscientific Model Development, 11, 1377-1403, https://doi.org/10.5194/gmd-11-1377-2018, 2018.

Schwarz, H. R., Köckler, N.: Numerische Mathematik, Ed.7, Vieweg+Teubner, Wiesbaden, https://doi.org/10.1007/978-3-8348-9282-9, 2009.

Sellar, A. A., Jones, C. G., Mulcahy, J. P., Tang, Y., Yool, A., Wiltshire, A., O'Connor, F. M., Stringer, M., Hill, R., Palmieri, J., Woodward, S., de Mora, L., Kuhlbrodt, T., Rumbold, S. T., Kelley, D. I., Ellis, R., Johnson, C. E., Walton, J., Abraham, N. L., Andrews, M. B., Andrews,

T., Archibald, A. T., Berthou, S., Burke, E., Blockley, E., Carslaw, K., Dalvi, M., Edwards, J., Folberth, G. A., Gedney, N., Griffiths, P. T., Harper, A. B., Hendry, M. A., Hewitt, A. J., Johnson, B., Jones, A., Jones, C. D., Keeble, J., Liddicoat, S., Morgenstern, O., Parker, R. J., Predoi, V., Robertson, E., Siahaan, A., Smith, R. S., Swaminathan, R., Woodhouse, M. T., Zeng, G., and Zerroukat, M.: UKESM1: Description and Evaluation of the U.K. Earth System Model, J. Adv. Model. Earth Sy., 11, 4513–4558, https://doi.org/10.1029/2019MS001739, 2019.

Sellers, P.J., Berry, J.A., Collatz, G.J., Field, C.B., and Hall, F.G.: Canopy reflectance, photosynthesis, and transpiration. III. A reanalysis using improved leaf models and a new canopy integration scheme, Remote sensing of environment, 42(3), pp.187-216, https://doi.org/10.1016/0034-4257(92)90102-P, 1992.

Sellers, P.J., Randall, D.A., Collatz, G.J., Berry, J.A., Field, C.B., Dazlich, D.A., Zhang, C., Collelo, G.D., and Bounoua, L.: A revised land surface parameterization (SiB2) for atmospheric GCMs. Part I: Model formulation, Journal of climate, 9(4), pp.676-705,https://doi.org/10.1175/1520-0442(1996)009<0676:ARLSPF>2.0.CO;2, 1996.

Sellers, P.J., Tucker, C.J., Collatz, G.J., Los, S.O., Justice, C.O., Dazlich, D.A., and Randall, D.A.: A revised land surface parameterization (SiB2) for atmospheric GCMs. Part II: The generation of global fields of terrestrial biophysical parameters from satellite data. Journal of climate, 9(4), pp.706-737, https://doi.org/10.1175/1520-0442(1996)009<0706:ARLSPF>2.0.CO;2, 1996.

Sitch, S., Prentice, I. C., Smith, B., Cramer, W., Kaplan, J., Lucht, W., Sykes, M., Thonicke, K., and Venevsky, S.: LPJ- a coupled model of vegetation dynamics and the terrestrial carbon cycle, Doctoral dissertation, Institute of Plant Ecology, Lund University, Lund, 213 pp., https://doi.org/10.5194/BG-11-2027-2014, 2000.

Sitch, S., Smith, B., Prentice, I. C., Arneth, A., Bondeau, A., Cramer, W., Kaplan, J. O., Levis, S., Lucht, W., Sykes, M. T., Thonicke, K., Venevsky, S.: Evaluation of ecosystem dynamics, plant geography and terrestrial carbon cycling in the LPJ dynamic global vegetation model, Global Change Biology, 9, 161-185, 10.1046/j.1365-2486.2003.00569.x, 2003

Sitch, S., Friedlingstein, P., Gruber, N., Jones, S. D., Murray-Tortarolo, G., Ahlström, A., Doney, S. C., Graven, H., Heinze, C., Huntingford, C., Levis, S., Levy, P. E., Lomas, M., Poulter, B., Viovy, N., Zaehle, S., Zeng, N., Arneth, A., Bonan, G., Bopp, L., Canadell, J. G., Chevallier, F., Ciais, P., Ellis, R., Gloor, M., Peylin, P., Piao, S. L., Le Quéré, C., Smith, B., Zhu, Z., and Myneni, R.: Recent trends and drivers of regional sources and sinks of carbon dioxide, Biogeosciences, 12, 653–679, https://doi.org/10.5194/bg-12-653-2015, 2015

Smith, B., Prentice, I. C., and Sykes, M.: Representation of vegetation dynamics in modelling terrestrial ecosystems: comparison two contrasting approaches within European climate space, Global Ecology and Biogeography, https://doi.org/10.1046/j.1466-822X.2001.t01-1-00256.x, 2001.

Smith, B., Wårlind, D., Arneth, A., Hickler, T., Leadley, P., Siltberg, J., and Zaehle, S.: Implications of incorporating N cycling and N limitations on primary production in an individual-based dynamic vegetation model, Biogeosciences, 11, 2027-2054, https://doi.org/10.5194/bg-11-2027-2014, 2014.

Soo-Hyung, K., Lieth, J.H.: A Coupled Model of Photosynthesis, Stomatal Conductance and Transpiration for a Rose Leaf (Rosa hybrida L.), Annals of Botany, Volume 91(7), 771–781, https://doi.org/10.1093/aob/mcg080, 2003

von Bloh, W., Rost, S., Gerten, D., and Lucht, W.: Efficient parallelization of a dynamic global vegetation model with river routing, Environmental Modelling & Software, 25, 685-690, https://doi.org/10.1016/j.envsoft.2009.11.012, 2010.

Walker, A.P., Johnson, A.L., Rogers, A., Anderson, J., Bridges, R.A., Fisher, R.A., Lu, D., Ricciuto, D.M., Serbin, S.P., and Ye, M: Multi-hypothesis comparison of Farquhar and Collatz photosynthesis models reveals the unexpected influence of empirical assumptions at leaf and global scales. Glob Change Biol. 2021; 27: 804– 822. https://doi.org/10.1111/gcb.15366, 2020.